Waste Management 32 (2012) 482–497

Contents lists available at SciVerse ScienceDirect

Waste Management

journal homepage: www.elsevier.com/locate/wasman

Pollution profiles and physicochemical parameters in old uncontrolled landfills

M. Regadío [a,*], A.I. Ruiz [a], I.S. de Soto [a], M. Rodriguez Rastrero [a], N. Sánchez [b], M.J. Gismera [b], M.T. Sevilla [b], P. da Silva [b], J. Rodríguez Procopio [b], J. Cuevas [a]

[a] Department of Geology and Geochemistry, Faculty of Science, Autónoma University of Madrid, Campus Cantoblanco, C/Fco. Tomás y Valiente 7, 28049 Madrid, Spain
[b] Department of Analytical Chemistry and Instrumental Analysis, Faculty of Sciences, Autónoma University of Madrid, Campus Cantoblanco, C/Fco. Tomás y Valiente 7, 28049 Madrid, Spain

ARTICLE INFO

Article history:
Received 25 February 2011
Accepted 16 November 2011
Available online 12 December 2011

Keywords:
Landfill pollution
Clays
Natural liner
Leachate composition

ABSTRACT

The long-term effectiveness of the geological barrier beneath municipal-waste landfills is a critical issue for soil and groundwater protection. This study examines natural clayey soils directly in contact with the waste deposited in three landfills over 12 years old in Spain. Several physicochemical and geological parameters were measured as a function of depth. Electrical conductivity (EC), water-soluble organic carbon (WSOC), Cl^-, NH_4^+, Na^+ and exchangeable NH_4^+ and Na^+ were used as parameters to measure the penetration of landfill leachate pollution. Mineralogy, specific surface area and cationic-exchange capacities were analyzed to characterize the materials under the landfills. A principal component analysis, combined with a Varimax rotation, was applied to the data to determine patterns of association between samples and variables not evident upon initial inspection. The main factors explaining the variation in the data are related to waste composition and local geology. Although leachates have been in contact with clays for long time periods (13–24 years), WSOC and EC fronts are attenuated at depths of 0.2–1.5 m within the clay layer. Taking into account this depth of the clayey materials, these natural substrata (>45% illite–smectite-type sheet silicates) are suitable for confining leachate pollution and for complying with European legislation. This paper outlines the relevant differences in the clayey materials of the three landfills in which a diffusive flux attenuation capacity (A_c) is defined as a function (1) of the rate of decrease of the parameters per meter of material, (2) of the age and area of the landfill and (3) of the quantity and quality of the wastes.

1. Introduction

Composite liners comprising a polymeric geomembrane, a clay liner and a natural geological barrier are crucial components of landfill barrier systems designed to protect surface and groundwater. Technical requirements for landfills were established by European legislation throughout the last decade (e.g., 1999/31/EC, 1999; 2003/33/EC, 2002; 2008/1/EC, 2008 and 2008/98/EC, 2008) and tend toward a high level of environmental protection. Directive 1999/31/EC (1999) provides technical standards for the storage of waste in landfills to protect, preserve and improve the quality of the environment. Landfill sites should comply with these standards in the short and long terms.

The multi-barrier concept is one preventive measure. This approach uses consecutive liners that operate independently of one another and prevent the effects of waste deposits on the surrounding environment. Under a worst-case scenario, i.e., that all or some of the engineering measures used to contain the deposit fail and that the pollutants are released, the geological substratum is the final barrier to the migration of pollutants. Therefore, selecting proper locations for landfills is important. These locations should contain substrata that can act as geological, hydrochemical and natural barriers to ensure the confinement of released waste and pollutants (Bilitewski et al., 1997).

Directive 1999/31/EC (1999) establishes that, in the case of municipal waste (MW) landfills, this natural liner must have a hydraulic conductivity (K) of $\leqslant 10^{-9}$ m/s and a depth of $\geqslant 1$ m. From a physicochemical point of view, evaluating the long-term effectiveness of such a barrier is essential. In addition, the stability of the liner (e.g., potential changes in K) and its retention capacity for contaminants must be established (Frascari et al., 2004; Munro et al., 1997; Xie et al., 2009).

Abbreviations: A_c, attenuation capacity; CEC, cationic-exchange capacity; DS, dissolved solids; EC, electrical conductivity; Ex_cation, exchangeable cation; h, moisture; K, hydraulic conductivity; LMMOAs, low-molecular-mass organic acids; PC, principal component; PCA, principal component analysis; R_d, ratio decrease per metre deep of parameter X, averaged per landfills; Sol_ion, soluble ion; SSA, specific surface area; WSIC, water soluble inorganic carbon; WSOC, water soluble organic carbon.

* Corresponding author. Tel.: +34 914976709; fax: +34 914974900.
E-mail address: mercedes.regadio@uam.es (M. Regadío).

0956-053X/$ - see front matter © 2011 Elsevier Ltd. All rights reserved.
doi:10.1016/j.wasman.2011.11.008

Contaminants within a landfill take the form of leachates. The potential pollution caused by leachates is the result of several factors, including the release of ammonia, chlorinated and non-chlorinated organic compounds and heavy metal ions into the environment, all of which are toxic to living organisms (Baccini et al., 1987; Christensen et al., 2001; Kjeldsen et al., 1998).

The focus of this paper is to evaluate and compare the behavior of natural clay substrata used as natural barriers in three old landfills. Clay minerals are the natural materials with the lowest permeability as a result of their high specific surface area (SSA). The main objective here is to assess the depth at which natural attenuation of the main components of the pollution front occurs. Toward this end, we selected locations that lack geomembranes and have housed landfill operations for 10–20 years. These characteristics are important for evaluating the current requirements of the EU directive, particularly in light of the fact that there are few well-documented, full-scale leachate fronts, and these are known primarily from studies of sandy aquifers (Brun et al., 2002; Christensen et al., 1994; Islam et al., 2001; Marzougui and Ben Mammou, 2006; van Breukelen et al., 2004).

2. Materials and sampling

2.1. Materials and site description

The analyzed materials were natural clays that were in direct contact with landfill leachates. Three landfills that had no composite polymeric or engineered clay barriers within the landfill vessel were chosen. The studied landfills were denoted as L1, L2 and L3. L1 (NE Spain) has a surface area of 3 ha, received 78,000 t/year of mixed industrial and MW and was 23 years old at the time when the samples were taken. L2 (central Spain) occupies 20 ha, received solely MW (135,000 t/year) and was 24 years old. L3 (central Spain) occupies 36 ha, received 145,000 t/year of mainly MW and was 13 years old.

In all cases, leachates saturated the waste at least 1 m above the clay surfaces. These leachates were named for their corresponding landfill followed by an L (L1L, L2L and L3L) and were sampled and analyzed (Section 4.1).

L1 is a peri-urban landfill that was developed in a defunct clay quarry. The dominant lithology consists of Tertiary (Oligocene) clayey and silty materials. The landfill is within the natural topography (or a shallow excavation), which is characterized by low relief; the highest elevation in the NW (130 m) and the lowest in the SE (110 m) determine the drainage network. L1 is much lower in elevation than L2 and L3 (595–640 m and 640–680 m, respectively). Three boreholes were drilled in L1: L1B1, L1B2 and L1B3, in that order from the bottom to the top of a smoothly sloping area.

L2 is also located in an abandoned clay quarry. The lithology corresponds to Tertiary (Middle Miocene) brown clays with silt and gray-green, micaceous fine sand exhibiting a wavy morphology. The elevation (similar to L3) varies from 595 (N and W) to 640 m (S and E). Intermittent streams run from the SE to the NW in the area. The L2 boreholes (L2B1 and L2B2) were drilled at a similar elevation.

L3 is a peri-urban landfill located in an abandoned clay quarry. This landfill sits atop a substrate of Middle Miocene brown and gray clays and micaceous-arkosic sand. The topography is rolling, and the elevations vary between 640 and 680 m (similar to L2) and generally decline from the SE to the NW. Two boreholes (L3B1 and L3B2) were drilled, with L3B1 located lower in elevation. As a result of clay extraction and deposition, the original topographies of L2 and L3 were extensively modified over large areas before the landfills were installed.

Regarding the meteorology, L1 is in an area with a Mediterranean climate, receiving a mean annual rainfall of 650 mm with a minimum of 30 mm in July and a maximum of 90 mm in October. L2 and L3 are in an area with a Continental Mediterranean climate, receiving a mean annual precipitation of 400–430 mm with a minimum of 10–13 mm in August and a maximum of 52–60 mm in May (L2) and in November (L3). Temperatures are similar among the three landfills (an annual average of 14 °C, a monthly minimum of 5–6 °C in January and a monthly maximum of 24 °C in July).

2.2. Sampling

The clay barrier samples were obtained from cores extracted with a rotational drill. The drill penetrated the waste and extracted a continuous borehole 0.1 m in diameter and a maximum of 5 m in length. Basic information about the boreholes is shown in Table 1.

The cores were not contaminated by the mud used in the lubrication of the drilling head (Fig. 1a). To prevent cross-pollution, latex gloves were used while handling the cores, marking the depths or distributing the samples. The cores were immediately wrapped within an LDPE plastic film to preserve the moisture and were transported to the laboratory in HDPE calibrated boxes measuring 1 m × 0.5 m, which were divided into five longitudinal sections of

Table 1
Period of time of the borehole extractions, waste heights, borehole lengths and the number of samples collected.

Landfill	Borehole	Month	Waste thickness (m)	Borehole depth (m)	No. of samples
L1	B1	November	17	3	10
	B2		14	5	11
	B3		11	3.2	9
L2	B1	April	42	5	14
	B2		45	3.5	12
L3	B1	May	28	5	13
	B2		27	4.9	14

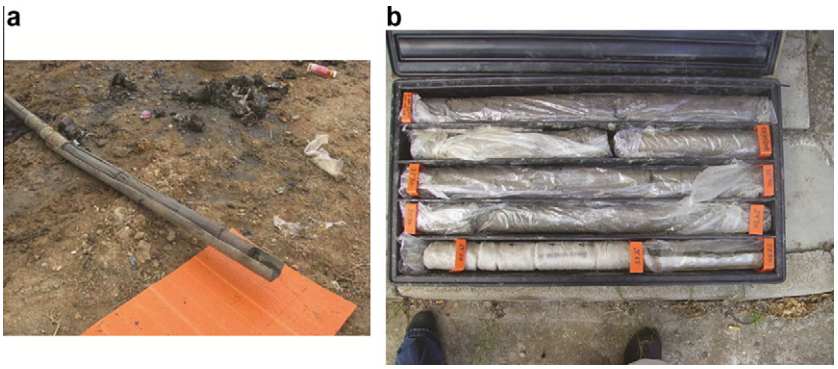

Fig. 1. (a) Appearance of a just-extracted core. (b) A core wrapped within a LDPE film and inside the transport box.

the same thickness as the cores (Fig. 1b). One core was transported per box, and the boxes were carefully closed and sealed.

Within the same day, the cylindrical cores were divided into samples of different thicknesses and from different depths (Appendix A: Tables A.1.1, A.2.1 and A.3.1). Beginning at the point of waste contact, the cores were sliced into four 0.025-m sections (samples M01, M02, M03 and M04) and subsequently into three or more consecutive sections measuring 0.05 m in thickness (M05, M06…). Another cylindrical section was taken at a depth of 0.75–1 m. Beginning at this depth, 0.10-m-thick sections were sampled by slicing every 1 m. Although the cores were not coated in drilling mud, the external surfaces of the samples were removed. The samples were preserved in the dark and were refrigerated (4 °C) until analyses were conducted.

The sampling of leachates was performed using piezometers or wells located near the boreholes. One liter was collected in opaque bottles with a pump and silicone tubing. The bottles were overflowed and closed with a Teflon hermetic top, making sure that no air was left inside. The instruments for each sampling were used only once.

3. Methods

3.1. Analyses of aqueous extracts

Physicochemical measurements of pH, redox potential and electrical conductivity were determined in duplicate at laboratory temperature in aqueous solutions from 10 g of solid sample (with a soil-to-deionized water ratio of 1:2.5) following methods published by the Ministerio de Agricultura, Pesca y Alimentación (1994). The solid samples used in these analyses and in the determinations of soluble carbon species and major soluble anions were first air dried for 7 days. pH was measured using a glass combined electrode calibrated with standard solutions of pH 4, 7 and 10. The redox potential was analyzed using a combined platinum electrode and calibrated using a 220-mV (pH 7, 25 °C) CRISON standard. Both parameters were measured in the supernatant that resulted from shaking the 1:2.5 solution for 10 min and allowing it to settle for 30 min. The solution was centrifuged and filtered through a polypropylene membrane with a pore size of 0.45 μm before measuring the EC with a multi-range cell (calibrated with potassium chloride standards).

The major soluble anions (primarily Sol_Cl^- and Sol_SO_4^{2-}) were determined by ion chromatography (METROHM™ 761 Compact IC) in an aqueous extract composed of a 1:10 soil-to-deionized-water ratio. The extracts were prepared from 2.5 g of sample and 25 mL of deionized water in sealed polypropylene centrifuge bottles, which were shaken for 24 h. The extracts were then centrifuged at 3500 rpm for 15 min, and 20 mL of the supernatant was filtered through a 0.45-μm membrane for analysis. Water-soluble carbon species were quantified in a Shimadzu® TOC-5000 carbon analyzer from aqueous solutions obtained using the same treatment as above but with a 1:5 solid-to-deionized-water ratio. The apparatus was calibrated with stock solutions of potassium hydrogen phthalate for water-soluble total carbon (WSTC) determination and with stock solutions of sodium hydrogen carbonate and sodium carbonate for water-soluble inorganic carbon (WSIC) determination. The water-soluble organic carbon (WSOC) content in the sample was determined by the difference between the WSTC and the WSIC.

Soluble cations and alkalinity were analyzed from an aqueous solution with a soil-to-deionized-water ratio of 1:10. The soil was obtained from the original refrigerated samples (without drying). The aqueous solutions were prepared by moisturizing 10 g of soil with 100 mL of water and allowing it to settle in a refrigerator for 24 h. Next, the solution was shaken for 24 h, centrifuged and passed through a 0.45-μm filter. Two replicates from each sample were measured. Sol_Na^+ and Sol_K^+ were analyzed using a Buck Scientific® PFP-7 flame photometer with 0.5, 1 and 2 mM Na/KCl stock solutions. Sol_Ca^{2+} and Sol_Mg^{2+} were determined using Flame Atomic Absorption Spectroscopy (Unicam™ Solaar M series atomic-absorption spectrometer) with 5, 15, 20, 30 and 40 mg/L Ca^{2+} stock solutions and 0.5, 0.75, 1, 1.5 and 2 mg/L Mg^{2+} stock solutions, respectively. Sol_NH_4^+ was estimated using an ion-selective potentiometer (ORION® 9512 Ammonia Gas Sensing Electrode) with 10^{-1}, 10^{-2}, 10^{-3}, 10^{-4} and 10^{-5} mol/L stock solutions. Alkalinity was determined by titration with an ORION® 960 potentiometer using a normalized H_2SO_4 solution (between 10^{-3} and 10^{-2} M) as the titrant and a pH meter to obtain the titration curve. The endpoint of the titration is the minimum point on a plot of the derivative of the pH *vs.* the volume of the consumed titrant (corresponding to a pH value ≈4.8).

To avoid any alteration of the original conditions, and particularly to avoid the modification of alkalinity or aqueous NH_4^+ by a previous heating treatment, these liquid extracts were obtained from wet samples.

3.2. Characterization of the solids

The solids remaining after the extraction of the soluble cations and alkalinity were used to determine the exchangeable cations (Ex_NH_4^+, Ex_Na^+, Ex_K^+, Ex_Ca^{2+}, Ex_Mg^{2+}) and the cationic-exchange capacity (CEC). The exchangeable cations were extracted at room temperature from 10 g of the original wet clay to a 100-mL solution, as described by Thomas (1982). Ex_Na^+, Ex_K^+, Ex_Ca^{2+} and Ex_Mg^{2+} were replaced by NH_4^+ homoionization after three cycles of shaking and centrifugation of the soil in contact with 25 mL of NH_4Ac, 1 M and pH = 7. After each cycle, the supernatant was poured into a 100-mL volumetric flask, which was then filled with deionized water (≈25 mL). The suspension was filtered through a 0.45-μm filter. The Ex_NH_4^+ was extracted in the other 10-g replicate from the soluble species. In this case, the soil was homoionized with Na^+, repeating three cycles of stirring and centrifugation with a dilution of 25 mL of 1 M NaAc at pH = 8.2. After each cycle, the supernatant was transferred into a 100-mL volumetric flask, and deionized water was added until the graduation mark (≈25 mL). Again, the solution was filtered. The exchangeable cations were analyzed using the same procedures described for the soluble-ion determinations.

The CEC was determined in the remaining solid after the Ex_NH_4^+ extraction. The additional Na^+ not present in the exchangeable sites was removed by successive washings in 100% ethanol until the measured EC was <30 μS/cm. The Na^+ was then displaced by Mg^{2+} with a $Mg(NO_3)_2{\cdot}5H_2O$ solution (0.5 M, pH = 5) at room temperature (Rhoades, 1982). The final Na^+ concentration was equivalent to the CEC and was measured in the previously mentioned flame photometer.

To reference these data and the liquid solution data (Section 3.1) with respect to the dry solid-sample mass, the gravimetric water content was also measured in duplicate. A 5-g portion of the original sample was weighed to an accuracy of ±0.01 g (m_m). The same fraction was weighed again after being dried at 105 °C for 48 h (m_d). Moisture (h) was estimated using the following formula:

$h = (m_m - m_d)/m_d \cdot 100$ (Ministerio de Agricultura, Pesca y Alimentación (1994))

The samples dried at 105 °C were mechanically ground at a frequency of 20/s for 5 min using a Retsch MM200 grinder to obtain a homogeneous particle size for specific-surface and global-mineralogy analyses. For the clay-mineralogy analysis, sections were taken from the original wet samples.

The SSA was measured in duplicate. Approximately 0.20 g of the ground material was then dried at 90 °C for 24 h and degassed under an N_2 flow for 18 h at 90 °C (UNE 22-164-94) using a Micromeritics™ Flow-Prep 060 station. Finally, the material was

weighed to within 0.0001 g. The SSA was measured by the Brunauer-Emmett-Teller (BET) method of nitrogen gas adsorption. The measurement was carried out at 77 K using a Micromeritics® GEMINI V and standard analysis protocol software that obtains a five-point N_2 adsorption isotherm.

The X-ray powder diffraction (XRD) technique was applied for the mineralogy analyses, and the software DRXWIN® (Primo, 2001) was used to analyze the data. XRD was performed using a Philips X'Pert diffractometer with a Ni-filtered CuKα radiation ($\lambda = 0.15406$ nm). The diffractometer operated at 40 kV and 40 mA with a step size of 0.016 ° and a speed of 2 s/step. Although a 10% relative error was assumed for these semi-quantification methods, the comparative differences between samples could be observed when the pattern profiles were plotted together.

The random-powder method was applied to estimate the overall mineralogical composition of the pre-dried and ground samples. The semi-quantifications of the minerals were performed according to Schultz (1964). A small quantity of ZnO (0.1 g) was mixed as an internal standard with 1 g of the bulk-ground sample to compare and to verify the differences between the very similar random powder diffraction patterns observed (Srodon et al., 2001). The patterns were normalized with respect to the area of the ZnO reflection at 0.2475 nm in the original powder pattern. The X-ray intensities were recorded over a range of 3 to 70 2θ (°).

The oriented-slide method was used to determine the specific families of clay minerals from selected original samples. The estimation of the clay mineral content in the <2-μm fraction was performed as proposed by UNE 22-161-92 with the scattering correction factors of Barahona (1974). Clay mineralogy is reported in terms of mass percentage relative to the total mineral content in the sample. Three glass slides per sample were prepared with the <2-μm size fraction (saturated in Mg^{2+} solution). Each slide underwent a different process: (a) air drying (0.1:2 clay-to-deionized-water ratio), (b) drying for 2 h at 550 °C (0.1:2) and (c) glycerol solvation (0.1:2 clay-to-water + glycerol ratio), following Moore and Reynolds (1997). The XRD intensities were recorded over a range between 3 and 20 2θ (°).

3.3. Data treatment

A multivariate statistical procedure using *Statistical Package for Social Sciences,* SPSS 16.0© for WINDOWS (SPSS Inc., Chicago, IL 60606-6412, 2007) was performed. To study the differences between the landfills, a principal component analysis (PCA) was performed, followed by a Varimax rotation. The analysis consisted of transforming the possibly correlated variables into a smaller number of uncorrelated variables (called principal components or PCs) that could describe the behavior of all of the original variables. The Varimax rotation was applied to determine which main variables correspond with the PCs. This analysis reveals the internal structure of the data in such a way that the variance within the data is well explained and little information is lost. This technique facilitates the interpretation of all of the data and variables as well as the variation of the variables within the data. The variables considered included pH, Eh, EC, WSOC, WSIC, h, Sol_NH^{4+}, Sol_Na^+, Sol_K^+, Sol_Ca^{+2}, Sol_Mg^{2+}, Sol_Cl^-, alkalinity, Sol_SO_4^{2-}, Ex_NH_4^+, Ex_Na^+, Ex_K^+, Ex_Ca^{2+}, Ex_Mg^{2+}, CEC, sheet silicates, quartz, Na-feldspar, K-feldspar, calcite and dolomite content, SSA and depth.

4. Results

4.1. Leachates

Table 2 presents the analytical results obtained for the leachates. Dissolved oxygen is present in low concentrations in all of the leachates, which indicates anaerobic conditions and reducing redox potentials. The leachates are alkaline, except for sample L3L, which is slightly acidic. The EC varies between the different leachates: L2L has the greatest value, followed by L1L and, finally, L3L. The lower inorganic ion concentration of L3L relative to the concentrations of the other landfills explains the EC of L3L. Organic matter was measured as WSOC, which is found in high concentrations (>1200 mg/L), especially in L3L (Table 2).

Table 2
Chemical analyses of the landfill leachates.

Parameters (mg/L)	L1L	L2L	L3L
O_2 (mg/L)	n.d.	0.07	0.50
pH	7.20	7.90	6.70
EC (mS/cm)	12.97	31.00	4.12
WSOC (mg/L)	1260	1744	3360
Alkalinity	44,012	43,920	27,450
Cl^- (mg/L)	9850	5700	269
SO_4^{2-} (mg/L)	225	1790	<5
NH_4^+ (mg/L)	117	1786	160
Ca^{2+} (mg/L)	305	86	87
Mg^{2+} (mg/L)	280	465	19
K^+ (mg/L)	450	1250	95
Na^+ (mg/L)	7700	3800	195
Phenols mg/L	1456	1.30	13
Benzene	<0.5	0.01	0.83
Toluene mg/L	<0.5	0.19	0.81
Etilbenzene mg/L	<0.5	0.06	0.10
Xylene	<0.5	0.17	2.10
Cr mg/L	0.04	0.83	0.03
Pb	0.43	<0.10	<0.10
Zn mg/L	0.32	<0.02	0.10
Cd mg/L	<0.02	<0.02	<0.02

n.d.: Not detected.

The major inorganic ions Cl^-, Na^+, K^+, Ca^{2+}, Mg^{2+}, SO_4^{2-} and NH_4^+ are present in significant concentrations (Table 2). In all cases, the dominant component is the alkalinity, whose concentration is one order of magnitude higher than the next most concentrated species, Cl^- and Na^+. The alkalinity is mainly composed of organic acid anions, as HCO_3^- was estimated to contribute only 14, 6 and 2% of the total alkalinity of L1L, L2L and L3L, respectively. From this point on, L1L is observed to possess a compositional trend different from that of the other two leachates: L1L has more K^+, Ca^{2+} and Mg^{2+} than SO_4^{2-} and NH_4^+, whereas L2L and L3L have more significant quantities of NH_4^+ than K^+, Ca^{2+}, Mg^{2+} and SO_4^{2-}. L2L is the only studied landfill with a high concentration of SO_4^{2-}, i.e., much higher than the concentrations measured in L1L and L3L.

Xenobiotic organic compounds (except for phenol in L1L) and heavy metals (<1 mg/L) were found in low concentrations (Table 2). Thus, these compounds were not measured in the soil samples.

4.2. Mineralogy of the landfill substrata

The X-ray powder-diffraction patterns of the three studied landfills (Appendix A: Fig. A.1.1, Fig. A.1.3, Fig. A.2.1, Fig. A.2.3, Fig. A.3.1, Fig. A.3.3) show an average clay content of >45%, with quartz and calcite as the main accessory minerals. Table 3 displays the average mineralogy of the materials that were in contact with the waste for each landfill. The X-ray oriented-diffraction patterns (Appendix A: Fig. A.1.2, Fig. A.1.4, Fig. A.2.2, Fig. A.2.4, Fig. A.3.2, Fig. A.3.4) show that in the <2-μm size, illite (1.0 nm, non-expandable with glycerol solvation) is the predominant clay mineral, followed by smectite (an expandable mineral that changes its basal d-spacing from 1.4 to 1.8 nm under glycerol solvation) and a smaller fraction of kaolinite and/or chlorite (0.71 nm).

4.3. Leachate infiltration: pollution profiles and attenuation depths

The contaminants are considered to be "attenuated" here when the analyzed parameters (1) have a virtually null variation with

Table 3
The average mineralogical composition (mass %) of the landfill substrata.

Substrata	Sheet silicates				No sheet silicates					
L1	Illite	Smectite	Chlorite	∑	Quartz	Na–feldspar	K–feldspar	Calcite	Dolomite	Others
	25 ± 3	14 ± 5	8 ± 2	**47 ± 17**	28 ± 14	3 ± 1	2 ± 2	19 ± 7	1 ± 1	
L2	Illite	Smectite	Kln + Chl	∑	Quartz	Na–feldspar	K–feldspar	Calcite	Dolomite	Others
	35 ± 3	7 ± 5	6 ± 2	**48 ± 18**	43 ± 16	4 ± 2	3 ± 2	0 ± 0	1 ± 1	Sd <1, Hem <1
L3	Illite	Smectite	Chlorite	∑	Quartz	Na–feldspar	K–feldspar	Calcite	Dolomite	Others
	52 ± 2	15 ± 5	8 ± 3	**75 ± 25**	17 ± 19	3 ± 5	2 ± 3	2 ± 3	1 ± 1	

∑: sum of sheet silicates, Kln + Chl: Kaolinite & chlorite, Sd: siderite, Hem: hematite.

depth and (2) reach low levels with regard to the values measured at the waste contact. For clarity, "the initial value" of a parameter is this highest value measured at the waste contact, the "background value" of a parameter is the value that the parameter reaches when it is attenuated, and the "attenuation depth" is the distance in meters from the waste contact to the depth at which attenuation occurs.

The average values of the measured parameters, classified by depths, from the three landfills are shown in Table 4.

To evaluate the capacity of the natural liner to attenuate the migration of contaminants, the variations in the analyzed parameters *vs.* depth were depicted, assuming that the main hydraulic gradients are vertical (Marzougui and Ben Mammou, 2006; Munro et al., 1997; Straub and Lynch, 1982) or considering diffusion as the main transport process. *K* was measured using a test sample taken at an average depth of 0.6 m. The average *K* values were 0.6×10^{-9} m/s (L1), 2.5×10^{-9} m/s (L2) and 1.0×10^{-9} m/s (L3), which were low enough to assume the predominance of diffusion transport processes (GEOCISA and UAM,

Table 4
The means and standard deviations of measured parameters in the landfill substrata, classified by depth.

Variables	Depth (m)	L1[a]	L2	L3
pH	0–0.5	8.6 ± 0.1	9.0 ± 0.1	8.5 ± 0.1
	0.5–1.25	8.8 ± 0.2	8.8 ± 0.2	8.7 ± 0.1
	1.25–2	9.2 ± 0.1	9.0 ± 0.0	8.7 ± 0.4
	2–5	9.5 ± 0.3	8.9 ± 0.1	8.7 ± 0.2
Eh (mv)	0–0.5	107 ± 33	141 ± 20	153 ± 22
	0.5–1.25	153 ± 27	166 ± 14	177 ± 21
	1.25–2	201 ± 85	165 ± 0.0	164 ± 8
	2–5	166 ± 26	159 ± 12	161 ± 12
EC (mS/cm)	0–0.5	7.3 ± 2.4	1.5 ± 0.5	1.2 ± 0.4
	0.5–1.25	9.3 ± 4.8	1.2 ± 0.1	0.5 ± 0.2
	1.25–2	0.7 ± 0.1	1.0 ± 0.0	0.4 ± 0.2
	2–5	0.5 ± 0.3	1.1 ± 0.2	0.3 ± 0.1
WSOC (μg/g)	0–0.5	303 ± 139	304 ± 186	305 ± 250
	0.5–1.25	189 ± 147	58 ± 19	102 ± 59
	1.25–2	112 ± 19	98 ± 0.0	73 ± 26
	2–5	116 ± 24	112 ± 81	71 ± 25
WSIC (μg/g)	0–0.5	390 ± 436	272 ± 82	307 ± 177
	0.5–1.25	955 ± 892	87 ± 37	183 ± 86
	1.25–2	135 ± 8	84 ± 0	170 ± 87
	2–5	130 ± 56	98 ± 55	131 ± 70
h (%)	0–0.5	18.9 ± 5.2	21.6 ± 1.5	33.5 ± 7.5
	0.5–1.25	27.0 ± 6.1	17.1 ± 8.6	36.7 ± 8.6
	1.25–2	18.6 ± 3.5	21.6 ± 0.0	29.7 ± 14.2
	2–5	15.4 ± 3.6	23.2 ± 3.7	31.2 ± 7.1
Sol_NH_4^+ (mmol/kg)	0–0.5	8.1 ± 2.3	40 ± 24	39 ± 32
	0.5–1.25	5.6 ± 5.0	3.8 ± 3.4	5.3 ± 7.6
	1.25–2	0.2 ± 0.3	2.6 ± 0.0	2.1 ± 2.9
	2–5	0.1 ± 0.2	4.4 ± 4.2	1.1 ± 0.9
Sol_Na^+ (mmol/kg)	0–0.5	246 ± 93	30 ± 10	19 ± 5
	0.5–1.25	311 ± 198	14 ± 7	10 ± 2
	1.25–2	22 ± 3	9 ± 0	7 ± 2
	2–5	17 ± 10	16 ± 6	6 ± 3
Sol_K^+ (mmol/kg)	0–0.5	5.7 ± 1.5	8.8 ± 4.2	8.3 ± 5.5
	0.5–1.25	4.1 ± 2.5	2.5 ± 0.4	1.6 ± 0.8
	1.25–2	0.7 ± 0.0	2.1 ± 0.0	1.5 ± 0.3
	2–5	0.9 ± 0.3	2.4 ± 1.3	1.6 ± 0.7
Sol_Ca^{2+} (mmol/kg)	0–0.5	7.5 ± 1.4	9.2 ± 15.3	5.1 ± 2.5
	0.5–1.25	8.5 ± 6.9	11.2 ± 9.3	5.4 ± 1.9
	1.25–2	3.5 ± 2.0	18.1 ± 0.0	5.1 ± 1.8
	2–5	3.6 ± 1.3	14.8 ± 15.6	5.1 ± 2.7
Sol_Mg^{2+} (mmol/kg)	0–0.5	8.8 ± 10.0	3.1 ± 2.5	7.1 ± 3.8
	0.5–1.25	8.5 ± 10.4	4.7 ± 1.3	8.5 ± 2.2
	1.25–2	2.8 ± 0.3	6.4 ± 0.0	8.2 ± 4.5
	2–5	2.3 ± 0.4	5.7 ± 1.3	8.9 ± 4.4
Sol_Cl^- (mmol/kg)	0–0.5	388 ± 128	14.1 ± 4.8	10.7 ± 7.3
	0.5–1.25	419 ± 258	7.9 ± 4.4	6.9 ± 2.2

Table 4 (*continued*)

Variables	Depth (m)	L1[a]	L2	L3
	1.25–2	26.5 ± 25	4.9 ± 0	4.4 ± 1.9
	2–5	8.2 ± 7.6	5.1 ± 2.1	2.6 ± 1.1
Alk (mmol/kg)	0–0.5	26 ± 7	53.8 ± 21.4	53.4 ± 27.4
	0.5–1.25	23 ± 8	12.5 ± 3.5	26.9 ± 15.4
	1.25–2	15 ± 2	12.2 ± 0	23.7 ± 12.6
	2–5	10 ± 1	12.2 ± 6.6	23.6 ± 13.3
Sol_SO_4^{2-} (mmol/kg)	0–0.5	2.2 ± 4.3	4.9 ± 2.0	0.7 ± 0.8
	0.5–1.25	10.2 ± 5.7	9.9 ± 1.4	0.2 ± 0.1
	1.25–2	1.0 ± 1.4	9.1 ± 0.0	0.1 ± 0.1
	2–5	0.2 ± 0.4	11.1 ± 1.7	0.2 ± 0.2
Sol_F^- (mmol/kg)	0–0.5	2.0 ± 1.5	n.d.	n.d.
	0.5–1.25	2.6 ± 2.3	n.d.	n.d.
	1.25–2	0.4 ± 0.2	n.d.	n.d.
	2–5	0.2 ± 0.1	n.d.	n.d.
Ex_NH_4^+ (cmol(+)/kg)	0–0.5	0.48 ± 0.10	2.8 ± 1.6	3.7 ± 2.5
	0.5–1.25	0.46 ± 0.27	0.4 ± 0.3	1.1 ± 1.5
	1.25–2	0.05 ± 0.07	0.1 ± 0.0	0.5 ± 0.7
	2–5	0.00 ± 0.08	0.3 ± 0.2	0.3 ± 0.2
Ex_Na^+(cmol(+)/kg)	0–0.5	3.6 ± 2.1	1.01 ± 0.37	0.69 ± 0.26
	0.5–1.25	5.5 ± 2.4	0.40 ± 0.24	0.23 ± 0.22
	1.25–2	1.1 ± 0.5	0.05 ± 0.00	0.41 ± 0.47
	2–5	0.7 ± 1.1	0.34 ± 0.31	0.19 ± 0.17
Ex_K^+(cmol(+)/kg)	0–0.5	0.62 ± 0.30	0.99 ± 0.44	1.41 ± 0.64
	0.5–1.25	0.79 ± 0.38	0.37 ± 0.08	0.69 ± 0.13
	1.25–2	0.31 ± 0.02	0.25 ± 0.00	0.54 ± 0.37
	2–5	0.33 ± 0.11	0.35 ± 0.23	0.47 ± 0.22
Ex_Ca^{2+}(cmol(+)/kg)	0–0.5	32.8 ± 7.8	17.1 ± 9.3	21.2 ± 9.6
	0.5–1.25	39.9 ± 10.6	11.5 ± 4.4	23.7 ± 2.5
	1.25–2	50.6 ± 8.6	6.1 ± 0.0	17.7 ± 12.5
	2–5	42.9 ± 2.9	13.9 ± 6.5	13.9 ± 11.0
Ex_Mg^{2+}(cmol(+)/kg)	0–0.5	5.8 ± 2.0	10.5 ± 3.4	22.1 ± 8.4
	0.5–1.25	13.4 ± 5.3	11.2 ± 3.6	27.3 ± 5.3
	1.25–2	19.7 ± 0.7	6.6 ± 0	23.5 ± 17.8
	2–5	11.9 ± 7.1	9.1 ± 6.3	16.9 ± 11.0
CEC (cmol (+)/kg)	0–0.5	10.6 ± 3.8	10.6 ± 2.5	30.2 ± 15.6
	0.5–1.25	20.8 ± 3.9	9.0 ± 4.0	34.4 ± 13.7
	1.25–2	22.8 ± 0.3	3.2 ± 0.0	13.6 ± 8.9
	2–5	13.4 ± 10.1	6.8 ± 4.9	11.2 ± 6.9
Sheet silicates (m %)	0–0.5	32 ± 9.40	55 ± 13.40	77 ± 23.29
	0.5–1.25	58 ± 14.15	47 ± 15.36	95 ± 1.63
	1.25–2	62 ± 2.47	23 ± 0	66 ± 42.14
	2–5	45 ± 26.65	35 ± 23.08	65 ± 29.29
Quartz (m %)	0–0.5	41 ± 12.70	37 ± 12.10	14 ± 17.18
	0.5–1.25	17 ± 3.98	43 ± 14.85	4 ± 2.05
	1.25–2	19 ± 0.85	67 ± 0	25 ± 33.73
	2–5	32 ± 21.29	54 ± 20.71	24 ± 23.38
Na-Feldspar (m %)	0–0.5	4 ± 1.90	3 ± 1.53	3 ± 5.18
	0.5–1.25	2 ± 0.73	5 ± 2.72	1 ± 0.50
	1.25–2	2 ± 0.57	5 ± 0	2 ± 2.69
	2–5	3 ± 0.55	5 ± 2.02	4 ± 5.24
K-Feldspar (m %)	0–0.5	4 ± 2.80	3 ± 1.79	2 ± 1.70
	0.5–1.25	1 ± 0.22	3 ± 2.14	1 ± 0.14
	1.25–2	1 ± 0.21	5 ± 0	5 ± 6.58
	2–5	1 ± 0.67	4 ± 3.89	4 ± 3.31
Calcite (m %)	0–0.5	19 ± 6.10	<1 ± 0.55	2 ± 2.64
	0.5–1.25	21 ± 11.55	<1 ± 0.00	<1 ± 0.57
	1.25–2	14 ± 0.14	<1 ± 0	<1 ± 0.57
	2–5	18 ± 6.86	<1 ± 0.00	2 ± 3.62
Dolomite (m %)	0–0.5	0.1 ± 0.20	1 ± 1.01	1 ± 0.73
	0.5–1.25	1 ± 1.39	2 ± 1.66	<1 ± 0.50
	1.25–2	3 ± 3.54	<1 ± 0	1 ± 0.28
	2–5	1 ± 2.02	1 ± 1.01	1 ± 0.85
SSA (m^2/g)	0–0.5	11 ± 4.30	42 ± 13.15	69 ± 26.25
	0.5–1.25	24 ± 7.23	40 ± 23.23	92 ± 16.62
	1.25–2	31 ± 0.23	11 ± 0	64 ± 53.03
	2–5	20 ± 16.67	25 ± 28.94	48 ± 36.83

Eh: redox potential, EC: electrical conductivity, WSOC/WSIC: water soluble organic/inorganic carbon, h: moisture, CEC: cationic-exchange capacity, Alk: alkalinity, SSA: specific surface area, n.d.: not detected.

[a] L1B3 was not included as it was not affected by the leachate.

2010). Fig. 2 shows the material-characterization parameters (the percentages of sheet silicates and SSA on the top *X*-axis and CEC on the bottom *X*-axis); Fig. 3 presents the global-chemistry parameters (pH and EC on the top *X*-axis and WSOC on the bottom *X*-axis); and Figs. 4, 5 and 7 show the chemical parameters as soluble ions (Sol_Cl^-, Sol_NH_4^+ and Sol_Na^+) on the top *X*-axis and exchangeable cations (Ex_NH_4^+ and Ex_Na^+) on the bottom *X*-axis.

The sum of exchangeable cations often exceeded the total charge of the clay (CEC), as shown in Appendix A (Tables A.1.4,

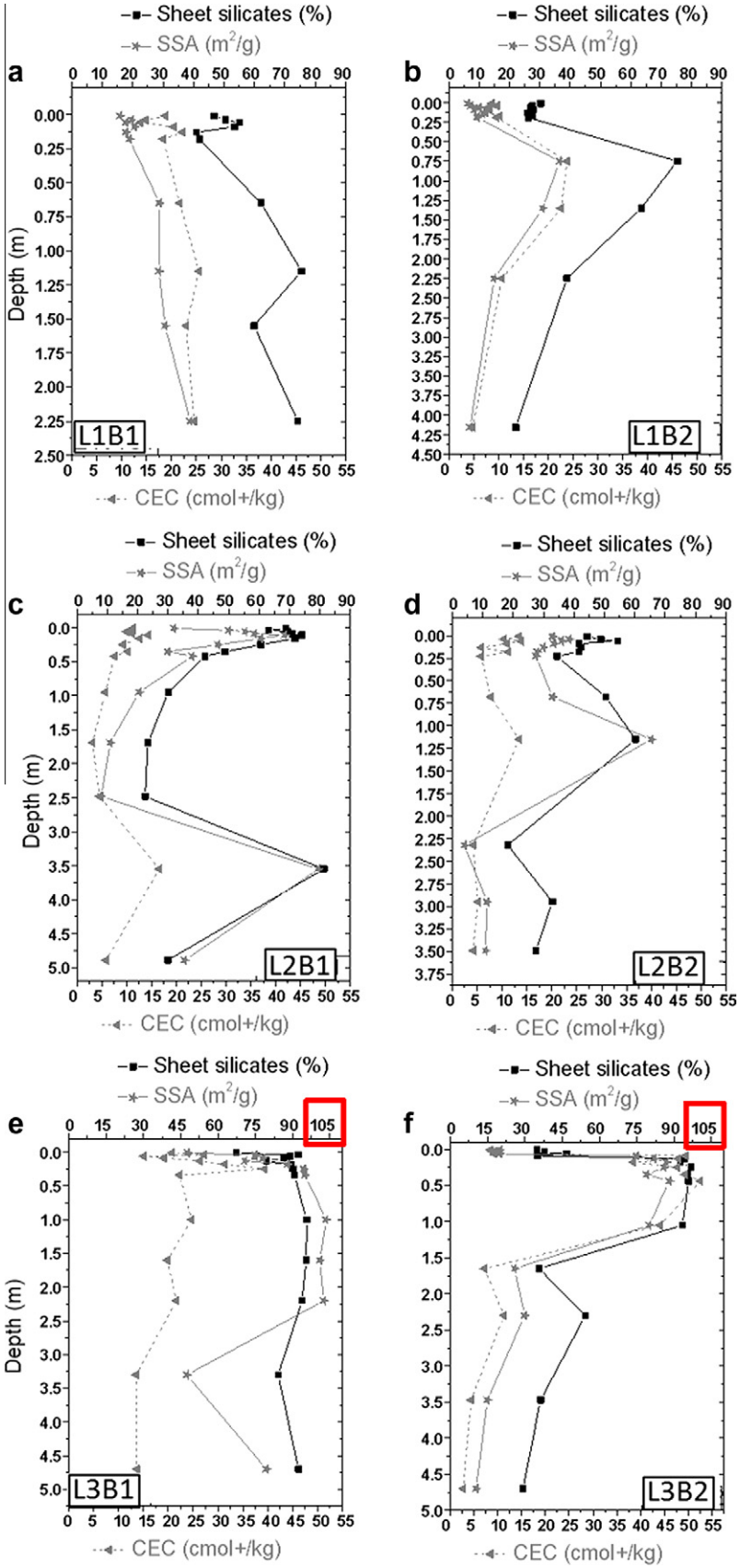

Fig. 2. Sheet-silicates content, specific surface area (SSA) and cationic-exchange capacity (CEC) profiles of (a) L1B1, (b) L1B2, (c) L2B1, (d) L2B2, (e) L3B1 and (f) L3B2.

A.2.4 and A.3.4). In all cases, this result was caused by the high concentrations of Ex_Ca^{2+} because the other exchangeable cations did not correspondingly increase. The higher the carbonate mineral content of the samples observed, the higher the measured

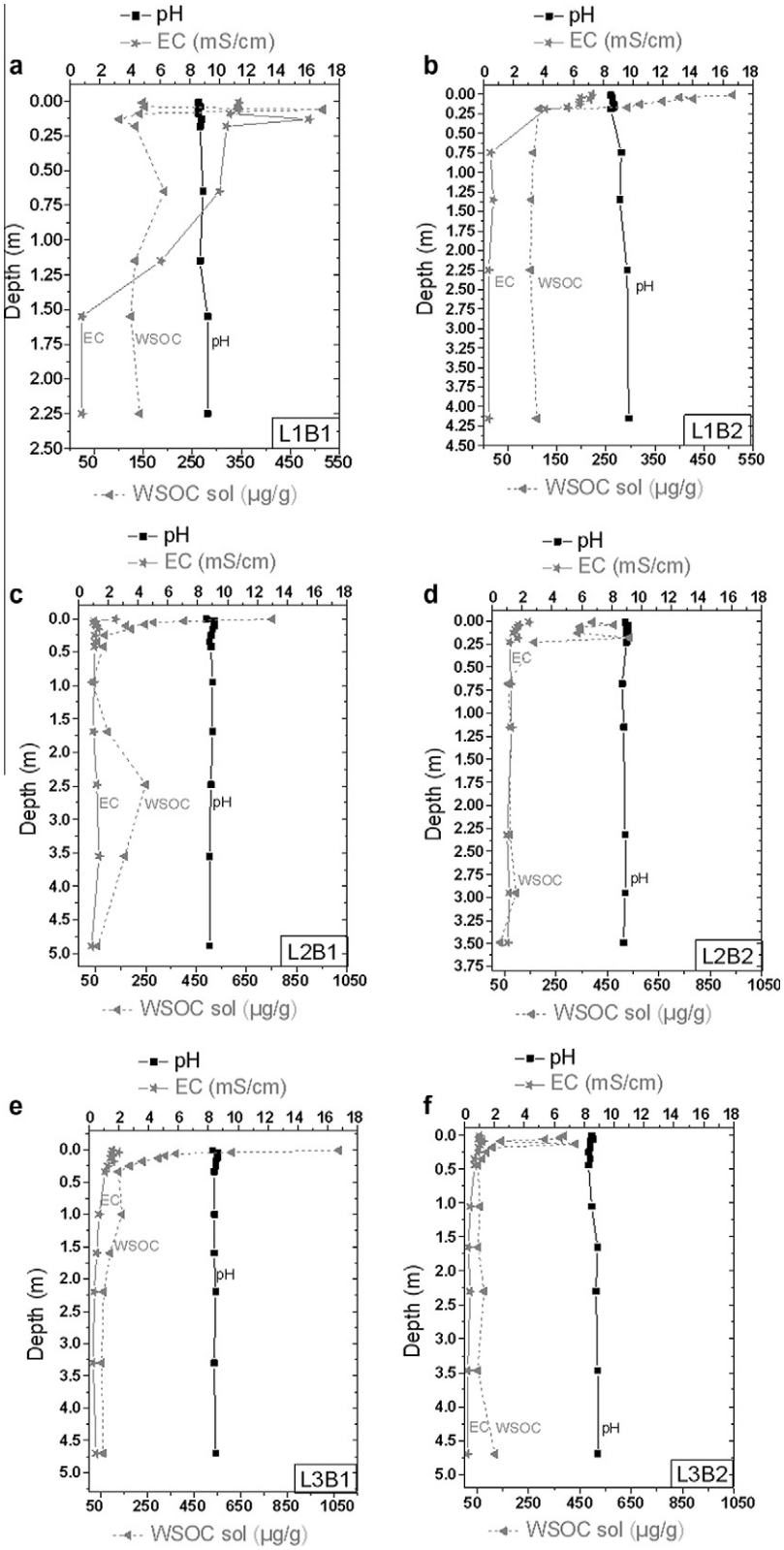

Fig. 3. pH, electrical conductivity (EC) and water soluble organic carbon (WSOC) profiles of (a) L1B1, (b) L1B2, (c) L2V1, (d) L2B2, (e) L3B1 and (f) L3B2.

concentration of Ex_Ca^{2+} and the more the sum of exchangeable cations exceeded the CEC (Appendix A). Therefore, these values were attributed to the dissolution of carbonate minerals during the analysis and not to the extraction of exchangeable cations. This is a common analytical artifact that cannot be directly resolved because it depends on the nature of the calcium minerals and their crystal size (Dohrmann, 2006; Dohrmann and Kaufhold, 2009).

4.3.1. L1

To characterize the different materials under the landfills, sheet-silicate content, SSA and CEC were studied along the profiles.

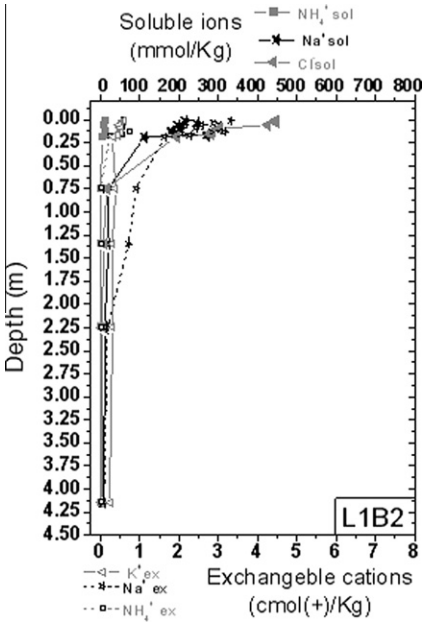

Fig. 4. L1B2 ion-profiles.

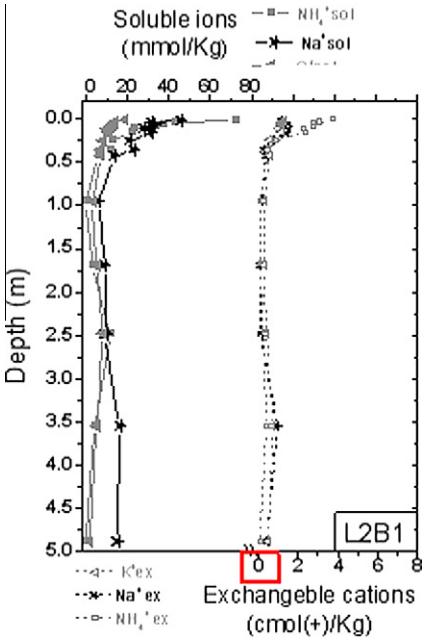

Fig. 5. L2B1 ion-profiles.

These parameters are positively related and contribute to the attenuation of pollutants.

The average values of sheet silicates, SSA and CEC of L1 substrata are 47 ± 17%, 20.5 ± 9.8 m^2/g and 16.7 ± 6.9 cmol(+)/kg, respectively. The L1B1 borehole shows an increase in these parameters with depth, whereas in L1B2, the values increase from 0 to 0.75 m, beyond which they begin to decrease (Fig. 2a and b). In the case of L1B3, sheet-silicate content, SSA and CEC decrease down to 0.63 m, then increase down to 1.45 m; from this depth onward, the material-characterization parameters stabilize at 50%, 25 m^2/g and 13 cmol (+)/kg, respectively.

The three boreholes of L1 present a rather homogeneous pH (Fig. 3a and b), with values of approximately 8.8 ± 0.3 that increase with depth in L1B1 (from 8.6 to 9.2) and L1B2 (from 8.5 to 9.7). This increase in pH is associated with the evolution from a shallow zone, which is especially affected by the landfill leachate, to a natural carbonate-clay material that determines the chemistry at increasing depths. WSOC becomes attenuated at a <0.19-m depth, with <150–100 μg/g in L1B1 and L1B2 (Fig. 3a and b). Lower values than these were measured at 0.013 m in L1B3. In fact, this borehole reaches background levels within the first few centimeters and assumes average values with respect the rest of the analyzed parameters that are very close to the background values of L1B1 and L1B2. The EC is attenuated at 1.55 m in L1B1 and at 0.75 m in L1B2, with values of 0.8 and 0.4 mS/cm, respectively (Fig. 3a and b). The EC from L1B3 samples is always <0.5 mS/cm.

The attenuation of EC is related to the decrease in the major ions of the landfill substratum (Sol_Na^+ and Sol_Cl^-, Fig. 4). These ions are attenuated in each borehole at the same depths as the EC. Indeed, both ions are the main soluble components of the landfill leachate (Table 2). In contrast, relatively low amounts of ammonium and organic components are present, and these are significantly reduced or diluted in the studied profiles (Fig. 3a and b, Fig. 4). Regarding the exchangeable cations, high concentrations of Ex_Na^+ were measured in the shallowest samples: 7.8 and 3.3 cmol(+)/kg in L1B1 and L1B2, respectively. These concentrations fall to background values of 1.4 (at 1.55 m in L1B1) and 0.2 (at 1.55 m in L1B2) cmol(+)/kg. The attenuation depth for Ex_Na^+ is the same as that for the soluble ions (1.55 m) in L1B1. In the case of L1B2 (Fig. 4), the Ex_Na^+ is attenuated at a greater depth (1.55 m) than the soluble ions (0.75 m). As a result of the unpolluted nature of L1B3, both soluble and exchangeable ion values have low concentrations along the entire profile (<5 mmol/L for Sol_Na^+ and <0.2 cmol(+)/kg for Ex_Na^+).

The L1B1 samples have higher salt concentrations than the L1B2 samples, whereas those of L1B2 are higher than those of L1B3. As indicated in Section 2.1, L1B1, L1B2 and L1B3 have decreasing waste thicknesses and leachate heads from L1B1 (bottom of the slope) to L1B3 (top of the slope). Indeed, L1B3 presents the characteristic properties of the undisturbed clay substrata.

4.3.2. L2

Sheet-silicate content, SSA and CEC in L2 are 48 ± 18%, 36.4 ± 19.8 m^2/g and 9.2 ± 3.7 cmol(+)/kg, respectively. Despite having a higher sheet-silicate content and, in particular, a higher SSA than the L1 substratum, the CEC is much lower (Fig. 2a, b, c and d). The L2 CEC values exhibit the least variation along the vertical profiles among the three locations. L2B1 shows high values of sheet silicates, SSA and CEC in the first 0.11 m, which quickly diminish. Next, at 3.55 m, the maximum values of these parameters are observed (Fig. 2c). In L2B2, these variables increase to a depth of 1.15 m and then decrease at a more rapid rate to a depth of 2.32 m, where they become constant (Fig. 2d). The clay-mineral distributions in L2 show two heterogeneous, less clayey layers (Fig. 2c and d). The first layer begins from the point of contact and rapidly evolves to a more clayey section (from 63 to 74% sheet silicates in L2B1 and from 44 to 54% sheet silicates in L2B2). This more-clayey and narrow section is immediately followed by a decrease in sheet-silicate contents that affects greater thicknesses (3.4 m in L2B1 and 1.1 m in L2B2). At these depths (3.5 and 1.15 m in L2B1 and L2B2, respectively), a clay-rich material appears again (81% sheet silicates in L2B1 and 60% sheet silicates in L2B2).

The two boreholes of L2 show pH values of approximately 8.9 ± 0.1, with the highest pH found at the point of waste contact (Fig. 3c and d). WSOC attenuation is observed at 0.95 and 0.68 m for L2B1 and L2B2, respectively, with background values of 50 μg/g (Fig. 3c and d). Unlike in L1 (in which the EC is attenuated after WSOC), in L2, EC attenuation (1.1 mS/cm) took place at 0.25

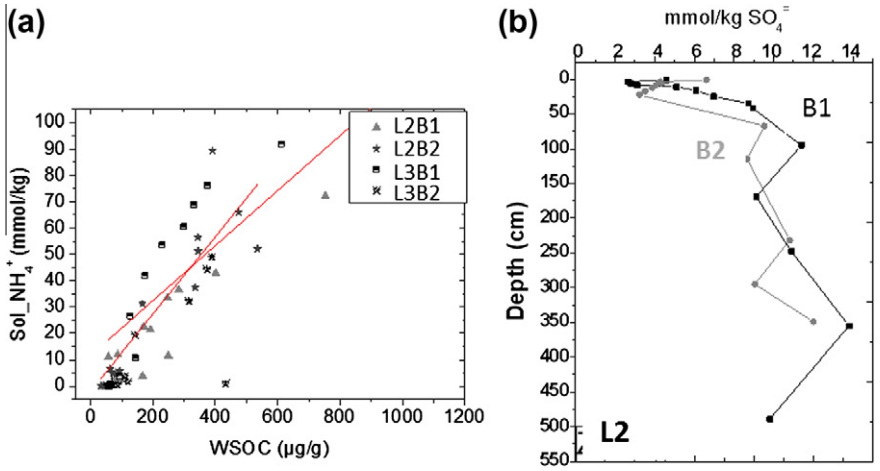

Fig. 6. (a) Lineal correlation between Sol_NH_4^+ and water soluble organic carbon (WSOC). (b) L2 sulphate-profiles for B1 and B2 boreholes.

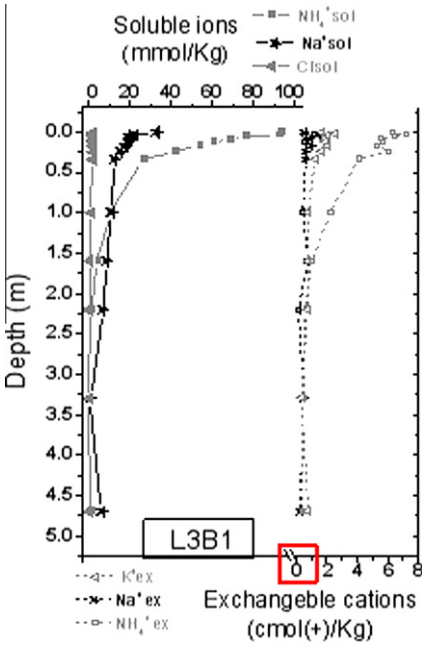

Fig. 7. L3B1 ion-profiles.

and 0.23 m for L2B1 and L2B2, respectively, i.e., approximately 0.70–0.45 m before the attenuation of WSOC. This is explained by the fact that the initial L2 EC values (2.5 mS/cm) are much lower than those in L1 (7–16 mS/cm). This suggests that WSOC, which is significantly higher in L2 (540–750 µg/g) than in L1 (510–515 µg/g), makes a small contribution to the value of the EC compared to the influence of inorganic soluble salts. WSOC increases locally in L2B1 at 2.5 m (Fig. 2c). At the same depth, the minimum sheet-silicate content and specific-surface values were found (Fig. 2c). This layer of material is presumed to have a higher permeability and lower retention capacity than the materials that are found above (0–0.5 m with an average K of 3×10^{-9} m/s) and below (>3.5 m). Thus, the transport of pollutants related to lateral hydraulic flows cannot be disregarded.

The attenuation of both soluble and exchangeable cations (Fig. 5) is observed at 0.95 and 1.15 m in L2B1 and L2B2, respectively. Although the ions in L2B2 extend further than the WSOC, at the point at which the WSOC was attenuated (0.68 m), these ions are reduced by >90% in L2B2.

In L2B1, the same increase that is observed for WSOC (Fig. 3c) can be observed for NH_4^+ (Fig. 5), indicating that the main origin of the NH_4^+ of the substrate comes from the organic matter, as shown in Fig. 6a for L2 and L3. Ex_Na^+ and Ex_NH_4^+ exhibit similar behaviors along the depth profiles. Values of 3.7–6.5 cmol(+)/kg were measured in L2B1 and L2B2, respectively, at the point of waste contact for Ex_NH_4^+ and of 1.5 cmol(+)/kg for Ex_Na^+. The average value of the total CEC at the point of waste contact is 10–14 cmol(+)/kg for L2B1 and L2B2, respectively (Fig. 2c and d); these values are typical for the illitic mineral (Hang and Brindley, 1970) that composes the natural clay under this landfill (Table 3). In this case, at the point of waste contact, the cation-exchange complexes of the sheet silicates are mostly saturated with Ex_NH_4^+ and Ex_Na^+ (Appendix A: Table A.2.4). In contrast, after the attenuation depth of 1 m, the sum of these monovalent cations is less than 1 cmol(+)/kg. Although values as low as 4 cmol(+)/kg of total CEC were measured, at these depths, Ex_Ca^{2+} and Ex_Mg^{2+} dominate the exchange complex (Appendix A: Table A.2.4). The L2B1 borehole shows a relative increase in Ex_Na^+ at 3.5 m (Fig. 5). This increase is found at the same position as the maxima of sheet-silicate content, SSA and CEC (Fig. 2c) and reflects the retention capacity of the clay minerals.

At the point of waste contact, the Sol_NH_4^+ concentration is much higher than that of Sol_Na^+, whereas at depths of 3–4 m, the Sol_NH_4^+ concentrations are very low compared to those of Sol_Na^+. Furthermore, the Sol_Na^+ decreases by 79% relative to its concentration at the point of waste contact, and the Sol_NH_4^+ decreases by 98%. This indicates that NH_4^+ is a typical signature of the leachate.

The lower quantity of sulfate in the first 0.35 and 0.68 m of L2B1 and L2B2, respectively, (Fig. 6b) coincides with the attenuation of the organic matter front (Fig. 3c and d). From these depths onward, WSOC is attenuated, and sulfate concentrations begin to increase. The oxidation of organic matter in the first centimeters may provide electrons to reduce the sulfate to sulfide. This reaction is common in the methanogenic stage of a landfill, when sulfate concentrations decrease in response to microbial reduction under strict anaerobic conditions (Kjeldsen et al., 2002; Lyngkilde and Christensen, 1992a, b).

Similar depth evolution parameters and values were measured at both boreholes, though L2B2 has a higher ion concentration than L2B1, in the shallowest samples. This finding is consistent with the thicker waste layer of L2B2 relative to that of L2B1 (Table 1) and with the longer attenuation distance of L2B2 relative to that of L2B1. Nevertheless, an unknown local change in the nature of waste may have an additional influence.

4.3.3. L3

L3 shows the highest values of sheet silicates, SSA and CEC of the three substrata, with averages of 75 ± 25%, 65.7 ± 30.7 m^2/g and 25.1 ± 15.7 cmol(+)/kg, respectively. However, the variation in the sheet silicates and the SSA along its profiles is also the highest, i.e., the difference between the maximum and minimum values is higher in L3 than in the other landfills. L3B1 has high values for both parameters along the profile to 3.3 m, where they drop under 50% and are then found in deeper samples (Fig. 2e). Likewise, CEC undergoes a slight decrease beginning at 1.6 m. These high initial values of sheet silicates, SSA and CEC in L3B1 are only present in L3B2 to 1.7 m. Beneath 1.7 m, they diminish by more than 60%, remaining constant in deeper zones (Fig. 2f). The minimum values are found in the first 0.05 m of both boreholes as a result of possible mixtures with non-clayey materials (Fig. 2e and f).

Samples from this landfill have pH values of approximately 8.5 ± 0.2. L3B2 shows a small increase in pH (8.3–8.9) toward the deepest samples (Fig. 3f). EC and WSOC at the point of waste contact are higher in L3B1 (2 mS/cm and 1017 μg/g) than in L3B2 (1.3 mS/cm and 430 μg/g), but their attenuation occurs at similar depths in L3B1 and L3B2. EC reaches background values (0.4–0.7 mS/cm) at 1 m and WSOC (background values of 52–130 μg/g) at 0.5 m (Fig. 3e and f). This depth corresponds to a great increase in the presence of clay (90% sheet-silicate contents; Fig. 2e and f). The higher (almost double) EC in L3B1 when compared to L3B2 (Fig. 3e and f) is related to the concentration of soluble ions (Fig. 7).

Ammonium is the predominant soluble cation (50–94 mmol/kg) and is complemented mostly by organic acid anions and bicarbonate alkalinity (Appendix A: Table A.3.3). The attenuation of Sol_NH_4^+ (4.1 mmol/kg at 1.60 m in L3B1 and 0.51 mmol/kg at 0.25 m in L3B2) follows the same pattern as EC attenuation. Sol_Na^+ is attenuated at 0.34 m (12.3 mmol/kg) and 0.44 m (10 mmol/kg) for L3B1 and L3B2, respectively. Ex_NH_4^+ diminishes from 7.2 to 0.5 cmol(+)/kg at 2.2 m in L3B1 and from 4.8 to <0.1 cmol(+)/kg at 0.44 m in L3B2. In L3B2 between 0.10 and 1 m, the sheet–silicate content is >92%, and the total CEC ranges between 45 and 50 cmol(+)/kg (Fig. 2f). These highly sorptive and clay-grade properties explain how Ex_NH_4^+ and Sol_NH_4^+ are attenuated at very short depths compared to L3B1, which has 80–90% sheet silicates and 20–30 cmol(+)/kg in total CEC (Fig. 2e). Both clayey materials contain a significant proportion of smectite (the mineral that mostly contributes to CEC) and show very high specific-surface values (80–90 m^2/g), which is consistent with the presence of montmorillonite smectites (Dogan et al., 2006).

L3B1 was drilled in a lower part of a slope than L3B2 (Section 2.1), receiving greater quantities of leachate and supporting more waste than L3B2. This is consistent with the fact that L3B1 has higher salt concentrations than L3B2.

4.4. Principal component analysis

PCA reduced the dimensionality of the data by diagonalizing the correlation matrix of the variables (Appendix B: Tables B.1 and B.2) and transforming the 28 variables into 28 uncorrelated (orthogonal) variables called principal components (PCs) (Appendix B: Table B.3). According to the criterion of Cattell and Jaspers (1967), 6 PCs out of the 28 were selected (Appendix B: Fig. B.1). These six PCs explain more than 80% of the variance. The loadings of the 28 variables on the 6 significant PCs calculated by PCA are shown in Appendix B: Table B.4.

A Varimax rotation was applied to highlight the participation of the variables that show higher contributions and to diminish the variables that show lower contributions. These calculations helped us to associate the correlated variables and to reduce the original large number of variables without losing too much information. The last column of Table 5 summarizes the variables that were grouped by each PC and the degree of correlation within the variables in each component (indicating the contribution of the variable within the PC). Thus, PC 1 explains 21.71% of the variance and is associated with 9 variables instead of the original 28. This PC is positively affected by moisture, Ex_Mg^{2+}, CEC, sheet-silicate content and SSA and negatively affected by pH, quartz, sodic-feldspar and potassic-feldspar.

Table 5
The principal components after the Kaiser Varimax rotation.

PC	Variance (%)	Variables (the correlation)	
		Negative correlation	Positive correlation
1	21.711	Quartz (−0.882) Na-Feldspar (−0.614) K-Feldspar (−0.566) pH (−0.553)	Sheet silicates (0.919) Ex_Mg^{2+} (0.918) SSA (0.877) h (0.819) CEC (0.814)
2	20.869		Sol_NH_4^+ (0.974) Alk (0.966) Sol_K^+ (0.963) Ex_NH_4^+ (0.941) Ex_K^+ (0.868) WSOC (0.818)
3	20.233		EC (0.965) Sol_Na^+ (0.962) Sol_Cl^- (0.953) Ex_Na^+ (0.935) WSIC (0.778) Calcite (0.728)
4	6.451	Ex_Ca^{2+} (−0.761)	Na-Feldspar (0.564)
5	6.157	Dolomite (−0.692) Eh (−0.529)	Sol_Mg^{2+} (0.633)
6	5.328		Sol_Ca^{2+} (0.727) Sol_SO_4^{2-} (0.720)

h: moisture, Ex_cation: exchangeable cation, CEC: cationic-exchange capacity, EC: electrical conductivity, Sol_ion: soluble ion, Alk: alkalinity, Eh: redox potential.

The focus of the analysis is on PCs 1, 2 and 3 because they account for more than 60% of the total variance. PC 1 is formed by the type of minerals and physicochemical parameters such as SSA, Ex_Mg^{2+}, pH and CEC. PC 1 is therefore related to geological information. PC 2 is affected by WSOC and the soluble and exchangeable species of ammonium, potassium and alkalinity, representing primarily the organic charge on the landfill substratum. PC 3 is the result of the combination of EC, sodium, chloride, WSIC and calcite, which explains inorganic soluble components and inorganic carbon. These PCs have similar variances because all of them group a similar number of correlated original variables, whereas the other PCs are formed by a lower number of correlated variables.

5. Discussion

5.1. Leachates

The interaction between a leachate and a geological barrier depends on a variety of factors, including leachate composition, which varies with (1) landfill age (i.e., the degree of waste stabilization), (2) landfill technology, (3) climate, (4) waste composition and (5) geological location (Chian and DeWalle, 1976; Christensen et al., 2001; Renou et al., 2008; Vadillo et al., 1999).

The three landfills are all mature (more than 10 years old) and use comparable containment technologies (no synthetic polymer-composite liners). Many studies have shown a relationship between the landfill age and the leachate chemical composition (Kulikowska and Klimiuk, 2008; Nanny and Ratasuk, 2002; Renou et al., 2008; Salem et al., 2008; Shouliang et al., 2008; Tatsi and Zouboulis, 2002). The pH increases with landfill age, whereas the chemical and biological oxygen demand (COD and BOD, respectively) and low-molecular-mass organic acid levels (LMMOAs)

undergo a rapid decrease during the first five years. Low BOD/COD ratios are typical of final anaerobic-methanogenic landfill stages (Banar et al., 2006; Chofqi et al., 2004; Ehrig, 1988; Renou et al., 2008; SWANA, 1997; Taylor and Allen, 2006). Electrical conductivity (EC) and dissolved solids (DS) also decrease with landfill age; however, as a result of the fluctuation of dry and wet seasons, these reductions occur over longer periods of time than do changes in COD, BOD or LMMOA. Table 6 shows the average values of leachate chemical parameters obtained from 25 different studies.

BOD and COD were not measured in the landfill leachates; therefore, no conclusions regarding the BOD/COD ratios can be made. The pH of L2L is consistent with the average pH calculated for mature landfills (>10 years old), whereas L1L and L3L leachates show pHs that are slightly less basic (Tables 2 and 6). This difference may be result from the continuous landfill operation that causes the mixing of old and new leachates. Nevertheless, older landfills tend to have leachates with higher pHs. Landfills L1 and L2 (23 and 24 years old, respectively) have higher leachate pH values (7.20 and 7.90, respectively) than L3L (13 years old and with a pH value of 6.70). The slightly acidic pH of L3L indicates that there are some areas in the landfill where the acetogenic stage has not yet been completed. This is common in landfills, where acetogenic and methanogenic stages usually occur simultaneously at different locations of the same landfill (Kjeldsen et al., 2002).

Over time, and as the stabilization of waste passes from the aerobic to the methanogenic stage, Eh decreases. During methanogenesis, CH_4 is increasingly produced, indicating an important reducing environment with Eh < 0 mV (Banar et al., 2006; Taylor and Allen, 2006). This is not reflected in Table 6 as a result of the limited number of data found during the literature review for mature landfills (eight), which do not provide a consistent statistical base. Furthermore, if large volumes of water percolate through the landfill (e.g., rainfalls) and substrata have low permeability, Eh increases in response to the dissolved oxygen and oxidants provided by the water (Lee et al., 2006).

Regarding the climate and waste composition, L1 has a higher rainfall than L2 and L3, and this produces greater quantities of leachates. In fact, L1L has a lower WSOC and ammonium concentration than do the other leachates, which is likely related to the presence of higher amounts of leachate that is more diluted as a result of the high volumetric flow. However, L1L has higher concentrations of sodium and chloride than do the other landfills, which corresponds to the mixed urban and industrial waste that is received by L1 because industrial waste possesses less organic charge than MW (Barton et al., 1985). In contrast, L2 and L3 received mainly MW, which is related to the higher concentration of organic matter (WSOC) and lower concentrations of metals, than L1L (Table 2). Thus, the quality of waste is the factor that most influences the pollution profiles.

5.2. The mineralogy of landfill substrata

The three locations present the same type of non-sheet-silicate minerals but in different proportions. Quartz is the dominant mineral in all cases, found in every type of environment because it is very resistant to erosion, weathering, transport and sedimentation. The L1 substratum is made up of a significant concentration of carbonates (20%), especially calcite, whereas L2 and L3 have lower carbonate concentrations (1–3%). Calcite is relatively easy to dissolve at slightly acidic pH, releasing calcium and bicarbonate to the solution and increasing the porosity and, consequently, the *K*. However, because soil pHs were maintained under alkaline conditions in the three landfills (8–9), this potential effect was not detected. This buffering capacity seems to be favorable for the performance of the landfill substrata with respect to heavy metal migration, for instance. In addition, at these pH values, some trace heavy metals (such as those of Zn, Cu and Ni) and ions (Fe, Mn) are precipitated in the presence of carbonates (Mostbauer, 2003).

The sheet-silicate minerals in the three substrata are illite, smectite and chlorite; L2 also presents some kaolinite. The difference between the locations is the proportion of illite and smectite (Table 3). The ratios of illite to smectite in L1, L2 and L3 are 1.8, 5 and 3.5, respectively. L1 and L3 have similar smectite content, but L3 has double the illite content of L1. The clay minerals differ in their retention capacity, exhibiting a more or less charged surface to catch the dissolved contaminants in the leachates. Thus, the minerals that possess desirable characteristics for pollutant retention (i.e., high SSA and CEC) conform to the following order: smectite > illite $\geqslant$ chlorite $\sim$ kaolinite (Bergaya et al., 2006).

SSA (L3 > L2 > L1) varies mainly as a function of the sheet-silicate content. In general, it was observed that low values of SSA and of sheet-silicate led to attenuation at greater depths than those observed for high values of SSA and sheet-silicate contents.

5.3. Leachate infiltration: pollution profiles and attenuation depths

EC, WSOC and the main soluble-ion concentration of the corresponding leachate were used to define a general attenuation depth

Table 6
The average chemical compositions of characteristic parameters of leachates for different landfill ages: a review.

Landfill age	pH	EC (mS/cm)	SS (mg/L)	DS (mg/L)	NH_4^+ (mg/L)	Cl^- (mg/L)
New	7.0 ± 0.9	15.6 ± 7.7	1888 ± 1402	16204 ± 10882	2692 ± 3068	2966 ± 2213
No. samples	45	23	11	23	25	28
Medium	7.4 ± 0.6	17.9 ± 10.0	772 ± 287	32260 ± 26770	1267 ± 1476	3449 ± 3194
No. samples	35	22	3	21	33	25
Mature	7.7 ± 0.9	13.2 ± 9.7	704 ± 685	6804 ± 8572	644 ± 810	3970 ± 3236
No. samples	35	17	9	9	27	17

Landfill age	T (°C)	Redox (mV)	BOD (mg O_2/L)	COD (mg O_2/L)	BOD/COD
New	19.0 ± 5.9	60.1 ± 80.4	13001 ± 10672	25150 ± 20944	0.49 ± 0.30
No. samples	20	22	23	24	23
Medium	22.8 ± 7.6	85 ± 48.3	2621 ± 5143	7514 ± 8747	0.67 ± 1.79
No. samples	21	20	16	39	16
Mature	16.1 ± 6.5	208 ± 152.0	2181 ± 4364	6409 ± 11125	0.24 ± 0.21
No. samples	8	8	33	37	32

EC: electrical conductivity, S.S: suspended solids, D.S: dissolved solids, T: temperature, BOD/COD: biological/chemical oxygen demand.
The landfill age classification is based on Renou et al. (2008): New: <5 years, Medium: 5–10 years, Mature: >10 years.
Compiled from Banar et al. (2006), Cecen and Cakiroglu (2001), Chofqi et al. (2004), Depountis et al. (2009), El-Fadel et al. (2002), Kulikowska and Klimiuk (2008), Lobo and Tejero (2007), Marttinen et al. (2003), Meju (2000), Mohammadzadeh et al. (2005), Mor et al. (2006), Morillas et al. (2009), Nanny and Ratasuk (2002), Owen and Manning (1997), Renou et al. (2008), Salem et al. (2008), Sanchez-Chardi and Nadal (2007), Shouliang et al. (2008), Spagni et al. (2007), Statom et al. (2004), Swati et al. (2008), Tatsi and Zouboulis (2002), Tejero et al. (1991), Vadillo et al. (1999), Zairi et al. (2004).

at which most of the contaminants became naturally attenuated by the geologic barrier. The results are organized by landfills and boreholes in Table 7 and include the initial and background values and the percentage decrease. These data show, in general, that these natural clay layers located under the landfills represent an effective barrier to the migration of leachate contaminants, in agreement with other studies (Bellir et al., 2005; Chen et al., 2005; Frascari et al., 2004; Hermanns Stengele and Plötze, 2000; Joseph et al., 2003; Rowe et al., 1995; Techer et al., 2001; Thornton et al., 2001).

The average data (Table 7) show that these natural clayey layers located under the landfills represent a good barrier to the migration of the main leachate soluble contaminants, which in general terms, become attenuated in 0.2–2.2 m after 9–24 years of waste deposit. These depths are similar to the ones registered for Na^+ and Cl^- (up to 1.3 m) under a 15-year old MW landfill in Yanful et al. (1988); for Na^+, Cl^- and WSOC (1 m) also under a 15-year old MW landfill in Quigley et al. (1987) and for Cl^- (>0.83 m) and volatile organic compounds (0.15 m) under a 5-year old hazardous landfill in Johnson et al. (1989). In all cases, the substrata were natural clays. Lake and Rowe (2005) also presented short attenuation depths in the underlying compacted clay of a faulty geomembrane component of the composite liner system, during 14 years. In addition, they confirmed their results with a contaminant transport modeling. On the other side, deeper depths in clayey soils were estimated by Munro et al. (1997) (Cl^- > 6 m, Na^+&WSOC > 2 m), denoting the dominance of diffusion transport over advection and a non-fractured material within the three substrata presented in this paper.

The three natural clay layers presented a zone at a shallow depth at which the proportion of clay minerals was low, followed by a sharp increase in sheet silicates with depth (Fig. 2). This finding is presumably a result of the sands and silts deposited as tailings from the previous clay quarry activities. The leachates may have been transported laterally through these heterogeneous layers. This would affect the total amount of leachate potentially infiltrated through the underlined clay, but this does not invalidate the natural attenuation observed as a function of depth. The analyzed parameters become attenuated after penetrating the more clayey material (70% of sheet silicates in L1, 75% in L2B1, 60% in L2B2 and 90% in L3). That is not the case for the WSOC in L1, which was rapidly attenuated through the less clayey material (30–40% of sheet silicates) before reaching the clay-rich substratum below. This finding is explained by the higher rainfall at this site and the low content of organic charge, which accelerated the degradation processes of organic matter (Allen, 2001). The organic front (WSOC) is generally attenuated at a shorter distance (Table 7) than the inorganic front (EC and dominant ion). This is consistent with the rapid decrease of organic components in leachate, resulting from naturally induced organic matter degradation, compared to the slower decrease of EC and DS (Table 6).

The attenuation of all ions in L2 occurs at the same depth, whereas in L1(B2) and in L3, the cation that dominates the exchangeable sites migrates further than the soluble cation (Table 7). This is related to the high smectite content in both landfills (Table 3), a mineral that provides more positions for retaining cations in their negatively charged interlayer. As a consequence, the presence of characteristic cations in exchangeable sites can be taken as a reliable signature of the leachate penetration.

The main difference between boreholes of the same landfill is related to the waste thickness: the greater the waste thickness (Table 1), the higher the parameter values (Table 7). In some cases, waste-column thickness is also positively related to a deeper attenuation depth. In other cases, the attenuation depths are more closely related to the different mineralogies and physical–chemical properties of the substrata. In general, the differences between the attenuation depths of EC, WSOC and ions within the boreholes of the same landfill are not significant, except for the ions in L3 (1.6–2.2 m in L3B1 and 0.25–0.44 m in L3B2). L3B1 has a deeper layer of high SSA and sheet silicates that have retained cations at greater depths than L3B2 (Fig. 2e and f). In spite of this, L3B2 has effectively attenuated the cations because the defined attenuation depths (Table 7) are shallower than those of the clay-rich material (Fig. 2f). This case demonstrates the importance of implementing a high-quality mineral barrier.

The concentrations of the pollutants measured in the front below the landfills are expected to be proportional to the main components measured in the leachate; however, the L2 front breaks from the anticipated correlation with regard to EC values. Taking into account the fact that its analyzed leachate (L2L) has the highest EC (Table 2), the samples under this landfill exhibit very low conductivity (six times lower than that of the L1 samples, Fig. 3). This may be explained by the lateral migration of solutes through the poor clayey material through the uppermost detected in this substratum. A more detailed spatial study must be performed to confirm this possibility.

Finally, to compare the attenuation capacity of the three sites under similar conditions of time, leachate exposure or waste-column

Table 7
The initial and background values, attenuation depths, percentage decreases of EC, WSOC and characteristic ions of the pollution fronts by boreholes and by landfills.

Landfill	Bore-hole	EC			WSOC			Characteristic ion of the pollution front			
Main components in the leachate		Initial – background values	Depth	Decrease	Initial – background values	Depth	Decrease	Ion	Initial – background values	Depth	Decrease
L1	B1	16 – 0.8	1.55	95%	520 – 130	0.18	75%	Sol_Na^+	600 – 27	1.55	96%
12.97 mS/cm								Ex_Na^+	7.8 – 1.4	1.55	82%
9850 mg Cl^-/L	B2	7.2 – 0.4	0.75	94%	510 – 100	0.19	80%	Sol_Na^+	270 – 15	0.75	94%
117 mg NH_4^+/L								Ex_Na^+	3.3 – 0.2	1.55	94%
1260 mg WSOC/L											
7700 mg Na^+/L											
L2	B1	2.5 – 1	0.25	60%	750 – 50	0.95	93%	$Sol\_NH_4^+$	72 – 3	0.95	96%
31.00 mS/cm								$Ex\_NH_4^+$	3.7 – 0.1	0.95	97%
5700 mg Cl^-/L	B2	2.5 – 1	0.23	60%	540 – 50	0.68	91%	$Sol\_NH_4^+$	90 – 3	1.15	97%
1786 mg NH_4^+/L								$Ex\_NH_4^+$	6.5 – 0.1	1.15	98%
1744 mg WSOC/L											
L3	B1	2 – 0.7	1.00	65%	1070 – 130	0.50	88%	$Sol\_NH_4^+$	95 – 4	1.6	96%
4.12 mS/cm								$Ex\_NH_4^+$	7.2 – 0.5	2.2	93%
269 mg Cl^-/L	B2	1.3 – 0.4	1.00	69%	430 – 52	0.44	88%	$Sol\_NH_4^+$	50 – 0.5	0.25	99%
160 mg NH_4^+/L								$Ex\_NH_4^+$	4.8 – <0.1	0.44	98%
3,360 mg WSOC/L											
195 mg Na^+/L											

Table 8
Diffusive flux attenuation capacities (A_c) for EC, WSOC and dominant leachate ions by time of leaching, ton of deposited waste and surface area of the landfill vessel for each landfill.

Substrata	Age	W	R_d				A_c			
			EC	WSOC	Sol_cat	Ex_cat	EC	WSOC	Sol_cat	Ex_cat
L1	23	2.61	0.93	4.20	0.94	0.57	55.83	252.13	56.43	34.22
L2	24	0.68	2.51	1.16	0.93	0.94	40.58	18.85	15.10	15.34
L3	13	0.40	0.67	1.88	2.28	1.33	3.48	9.78	11.86	6.89

thicknesses, the following equation was developed and applied for each indicative parameter of Table 7. The objective was to normalize the data to define a comparable diffusive flux attenuation capacity (A_c) between landfills:

$$A_c = R_d \cdot Y \cdot W,$$

where R_d (m^{-1}) is the ratio decrease per meter depth of the indicative parameter, averaged per landfill. This was calculated as (percentage decrease/100)/attenuation depth. Y (years) is the age of the landfill at the time of sample collection. W ($t/y/m^2$) is the quantity of waste deposited per year and per unit of area.

Hence, the higher the A_c value, the better the barrier performance of the substratum. In Table 8, the three landfill sites are ranked from high to low A_c as follows: L1 > L2 > L3. The highest A_c corresponds to the substratum with the lowest K (0.6×10^{-9} m/s). This high A_c coefficient in L1 is in response to the greatest amount of deposited wastes compared to the area of the landfill vessel within the three landfills, i.e., W (Table 8). This causes the natural material of L1 to reduce its EC per meter of depth beyond that of L2 and ions per meter of depth beyond that of L3. L3 has the lowest A_c as a result of its shorter period of contact with the leachate pollution (it is 10 years younger than the other landfills) and the minor quantity of waste mass per unit of area (Table 8).

A greater A_c value was expected for this landfill because it was the one with the highest clay proportion with a high retention capacity (Table 3). Because the age component is positively factored into the A_c equation, a future study would be necessary to understand how the attenuation varies with time to generate confidence the usefulness of the A_c parameter. Thus, if the capacity to decrease the parameters per meter of L3 material does not change after 10 years, its A_c for EC, WSOC, Sol_cation and Ex_cation will be doubled. The defined coefficient may serve to compare old landfills in the absence of precise hydrological and hydrochemical data, but one must be careful not to distort the calculation with landfills of very different ages.

When comparing the two landfills of similar age (L1 and L2), even when L1 received almost four times as many tons of waste per hectare than L2 and the initial ion values of L1 (i.e., ions measured at the shallowest samples) were considerably higher than those of L2 (Table 7), there are no significant differences regarding the R_d values of the soluble species between these landfills (Table 8). Furthermore, the WSOC is more rapidly attenuated in L1 (diminishing 420% per meter) than in L2 (116% per meter) as a result of the lower initial WSOC and the higher precipitation in L1 than in L2, which increases the dilution and degradation of organic pollutants.

Following a discussion of the attenuation depth data, a hypothetical value for the K of the landfill substrata was estimated by applying a simplified ratio that assumes a hydraulic gradient of 1 and neglecting the existence of diffusion transport. This K is the average distance covered by the parameters, i.e., EC, WSOC, soluble and exchangeable ions (1.01, 0.79 and 0.93 m), divided by the landfill age (23, 24 and 13 years). The resulting values (1.4×10^{-9}, 1.0×10^{-9} and 2.3×10^{-9} m/s for L1, L2 and L3, respectively) are within an order of magnitude of the tested values. This provides confidence regarding the values of thickness (*depth*) and K of the natural liner under an urban landfill established by the Directive 1999/31/EC (1999) ($\geqslant 1$ m and $\leqslant 1.0 \times 10^{-9}$ m/s). Because some of the leachates may migrate through preferential pathways in the studied cases, these data may overestimate the attenuation capacity of the materials. Nevertheless, taking the results of this study into account, such conditions ensure waste retention for up to 24 years for the major soluble components of leachates when the landfill leachate is collected.

5.4. The interpretation of the principal component analysis

All of the PC scores that corresponded to each analyzed sample (Appendix B: Table B.5) were represented as pairs in a bivariate plot (1 axis per PC) and were then differentiated according to the three landfills. This procedure allowed for the observation that the geological PC 1 (Table 5) positively affects most of the samples of L1 and L3 (i.e., they are situated on the positive side of the PC 1-axis), whereas L2 samples are distributed along the negative side (Fig. 8a). Therefore, L1 and L3 have more sheet silicates (because they have less quartz), moisture, CEC, SSA and Ex_Mg^{2+} (consistent with the abundance of trioctahedral-Mg-sheet silicates in L3) than does L2. The fact that both L1 and L3 substrata decreased the

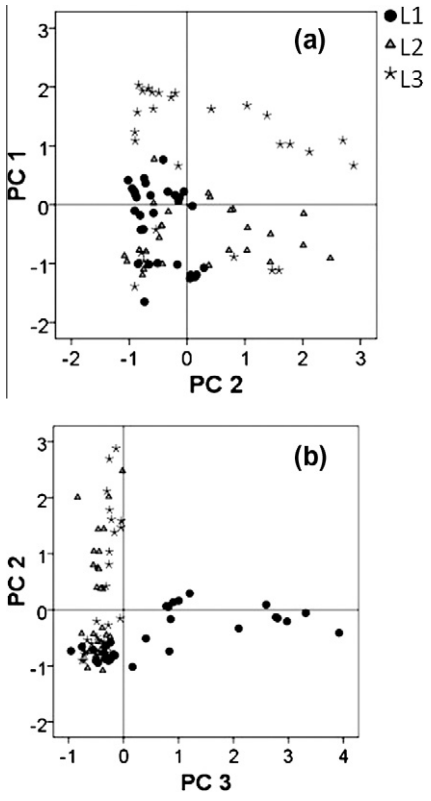

Fig. 8. Bivariate scatter plots of principal components scores from PC 1, 2 and 3 (Appendix B: Table B.5).

highest amount of WSOC, Sol_cation and Ex_cation at the shallowest depth, whereas L2 showed a minor retention capacity (R_d in Table 8), demonstrates that substrata with high values in the mineralogical and physicochemical parameters combined in PC 1 (Table 5) provide an effective barrier function. Therefore, the components integrating this PC are proposed as the most relevant parameters to be taken into account in defining the quality of optimum clay barriers in future studies.

PC 2, representing the organic related soluble species, influences L2 and L3 in the same way, but it does not affect L1 (Fig. 8a and b) for any of the PC-crossed combinations. In contrast, L1 samples were affected positively by PC 3 (inorganic soluble components) (Fig. 8b). Thus, both of these PCs (when they are plotted together in a graph) distinguish L1 from L2 and L3 (Fig. 8b). Clearly, PC 2 and PC 3 classify the landfills depending on their waste compositions: PC 2 affects urban-waste landfills, and PC 3 affects positively mixed industrial- and urban-waste landfills.

According to Table 5, MW produces a front with high contents of WSOC, alkalinity, ammonium and potassium and relatively low amounts of chloride. This is consistent with the MW leachate composition of landfills during the methanogenic stage determined by Jorstad et al. (2004). In contrast, the presence of industrial waste generates a leachate front that is characterized by high EC and high **leachate** chloride, sodium and inorganic carbon contents, which, in this case, are mainly attributed to calcite because L1 is the landfill with the highest calcite content (Table 3).

6. Conclusions

An approach to comparing the performance of the clay substrata of three old landfills was proposed through the analysis of pollution profiles, the calculation of attenuation depths and attenuation capacities (normalized by the parameter A_c) and the application of a principal component analysis (PCA). The studied features in the substrata indicate that small differences in the qualities of the clay mineral layer can influence the effectiveness of the *natural liner*, i.e., higher or lower A_c. Under similar sheet-silicate contents, the SSA (specific surface area) can vary considerably depending on the nature of the clay minerals. The presence of smectite, generally <15%, provides better protection for the environment by contributing SSA- and CEC-retention properties. This mineral can presumably have an added value for contaminant controlling because it acts as a "sensor" for monitoring cation pollution.

The presented data indicate that natural substrata with more than 45% sheet silicates of the illite–smectite type constitute an effective barrier to the migration of leachate contaminants. CEC, SSA and the buffering capacity of the clay substratum (pH 8–9) have been identified by the PCA analysis as relevant parameters to be considered in the characterization of an optimal geological barrier.

The average results from the different substrata showed that the EC diminished by 96% in 0.7 m, the WSOC decreased by 97% in 0.4 m, the soluble ion concentration (characteristic of the leachate) was reduced by 97% in 0.7 m and the exchangeable cation was reduced by 95% in 1 m. Taking into account these values and the average K of the three sites ($1.4{\cdot}10^{-9}$ m/s), the depth and the K of the natural liner established by Directive 1999/31/EC (1999) ($\geqslant$1 m and $\leqslant 1 \times 10^{-9}$ m/s) associated with adequate leachate collection and artificial sealing are adequate for the pollution control of major soluble species in the leachates.

Additionally, the data from the present study (Appendix A) can be used as a database to verify numerical modeling exercises developed to represent and reproduce leachate-component transport through underlying soils in uncontrolled landfills (Chen et al., 2005; Rowe et al., 1995).

Acknowledgements

This work was supported by the Spanish Environmental Ministry (MMA: I+D+i A113/2007/3_02.6) in cooperation with Geotecnia y Cimientos S.A. (GEOCISA) and the Centro de Experimentación de Obras Públicas (CEDEX).

Appendices A and B. Supplementary data

Supplementary data associated with this article can be found, in the online version, at doi:10.1016/j.wasman.2011.11.008.

References

UNE 22-161-92. Standard method for mineralogical quantification of clay samples containing sepiolite. 1992.
UNE 22-164-94. Standard method for BET specific surface determination in sepiolite-based materials. 1994.
1999/31/EC, O.J.L., 1999. Council Directive of 26 April 1999 on the ladfill of waste, European Union legislation.
2003/33/EC, O.J.L., 2002. Council Decision of 19 December 2002 establishing criteria and procedures for the acceptance of waste at landfills pursuant to Article 16 of and Annex II to Directive 1999/31/EC on the landfill of waste, European Union legislation.
2008/1/EC, O.J.L., 2008. Council Directive of 15 January 2008 concerning integrated pollution prevention and control, European Union legislation.
2008/98/EC, O.J.L., 2008. Council Directive of 19 november 2008 on waste and repealing certain directives, European Union legislation.
Allen, A., 2001. Containment landfills: the myth of sustainability. Engineering Geology 60, 3–19.
Baccini, P., Henseler, G., Figi, R., Belevi, H., 1987. Water and element balances of municipal solid-waste landfills. Waste management & research 5, 483–499.
Banar, M., Ozkan, A., Kurkcuoglu, M., 2006. Characterization of the leachate in an urban landfill by physicochemical analysis and Solid Phase Microextraction-GC/MS. Environmental Monitoring and Assessment 121, 439–459.
Barahona, E., 1974. Arcillas de ladrillería de la provincia de Granada: evaluación de algunos ensayos de materias primas. Granada University PhD, Spain.
Barton, J.R., Poll, A.J., Webb, M., Whalley, L., 1985. Waste Sorting and RDF Productions in Europe. Applied Science Publishers.
Bellir, K., Bencheikh-Lehocine, M., Meniai, A.H., Gherbi, N., 2005. Study of the retention of heavy metals by natural material used as liners in landfills. Desalination 185, 111–119.
Bergaya, F., Lagaly, G., Vayer, M. 2006. Cation and Anion exchange. In: Bergaya, F., Theng, B.K.G., Lagaly G. (Eds.), Handbook of Clay Science. Developments of Clay Science, vol. 1, 979–1001.
Bilitewski, B., Härdtle, G., Marek, K., Fischer, K.J., 1997. Waste Management. Springer.
Brun, A., Engesgaard, P., Christensen, T.H., Rosbjerg, D., 2002. Modelling of transport and biogeochemical processes in pollution plumes: Vejen landfill, Denmark. Journal of Hydrology 256, 228–247.
Cattell, R.B., Jaspers, J., 1967. A general plasmode (no. 30-10-5-2) for factor amalytic exercises and research. Multiple Behaviour Research Monographs 67, 1–212.
Cecen, F., Cakiroglu, D., 2001. Impact of landfill leachate on the co-treatment of domestic wastewater. Biotechnology Letters 23, 821–826.
Chen, Y.G., Zhang, K.N., Huang, C.B., 2005. Analysis on contaminants transport process through clay-solidified grouting curtain in MSW landfills. Journal Of Central South University Of Technology 12, 168–172.
Chian, E., DeWalle, F.B., 1976. Sanitary landfill leachates and their treatment. Journal of the Environmental Engineering Division-Asce 102, 411–431.
Chofqi, A., Younsi, A., Lhadi, E.K., Mania, J., Mudry, J., Veron, A., 2004. Environmental impact of an urban landfill on a coastal aquifer (El Jadida, Morocco). Journal of African Earth Sciences 39, 509–516.
Christensen, T.H., Kjeldsen, P., Albrechtsen, H.J., Heron, G., Nielsen, P.H., Bjerg, P.L., Holm, P.E., 1994. Attenuation of landfill leachate pollutants in aquifers. Critical Reviews in Environmental Science and Technology 24, 119–202.
Christensen, T.H., Kjeldsen, P., Bjerg, P.L., Jensen, D.L., Christensen, J.B., Baun, A., Albrechtsen, H.J., Heron, C., 2001. Biogeochemistry of landfill leachate plumes. Applied Geochemistry 16, 659–718.
Depountis, N., Koukis, G., Sabatakakis, N., 2009. Environmental problems associated with the development and operation of a lined and unlined landfill site: a case study demonstrating two landfill sites in Patra, Greece. Environmental Geology 56, 1251–1258.
Dogan, A.U., Dogan, M., Onal, M., Sarikaya, Y., Aburub, A., Wurster, D.E., 2006. Baseline studies of The Clay Minerals Society source clays: Specific surface area by the Brunauer Emmett Teller (BET) method. Clays and Clay Minerals 54, 62–66.
Dohrmann, R., 2006. Cation exchange capacity methodology III: Correct exchangeable calcium determination of calcareous clays using a new silver-thiourea method. Applied Clay Science 34, 47–57.
Dohrmann, R., Kaufhold, S., 2009. Three new, quick CEC methods for determining the amounts of exchangeable calcium cations in calcareous clays. Clays and Clay Minerals 57, 338–352.
Ehrig, H.J., 1988. Water and element balances of Landfills. In: Baccini, P. (Ed.), The landfill. Springer, Verlag, Berlin, Germany, p. 83.

El-Fadel, M., Bou-Zeid, E., Chahine, W., Alayli, B., 2002. Temporal variation of leachate quality from pre-sorted and baled municipal solid waste with high organic and moisture content. Waste Management 22, 269–282.
Frascari, D., Bronzini, F., Giordano, G., Tedioli, G., Nocentini, A., 2004. Long-term characterization, lagoon treatment and migration potential of landfill leachate: a case study in an active Italian landfill. Chemosphere 54, 335–343.
GEOCISA and UAM, 2010. ANEJOS DEL INFORME DE ACTIVIDADES DE ANUALIDAD 2007: Resultados de Ensayos geotécnicos y químicos (CEDEX). In: Informe final del proyecto: "La difusión de contaminantes en las barreras de vertederos urbanos y su evolución en el tiempo". Proyecto I+D+i - A 113/2007/03–02.6. Ministerio de Medioambiente, Rural y Marino, Gobierno de España. p. 114.
Hang, P.T., Brindley, G.W., 1970. Methylene blue absorption by clay minerals. Determination of surface areas and cation exchange capacities (Clay-organic studies XVIII). Clays and Clay Minerals 18, 203–212.
Hermanns Stengele, R., Plötze, M., 2000. Suitability of minerals for controlled landfill and containment. In: Vaughan, D.J., Wogelius, R. (Eds.). Environmental Mineralogy, EMU Notes in mineralogy, pp. 291–331.
Islam, J., Singhal, N., O'Sullivan, M., 2001. Modeling biogeochemical processes in leachate-contaminated soils: a review. Transport in Porous Media 43, 407–440.
Johnson, R.L., Cherry, J.A., Pankow, J.F., 1989. Diffusive contaminant transport in natural clay – A field example and implications for clay-lined waste-disposal sites. Environmental Science & Technology 23, 340–349.
Jorstad, L.B., Jankowski, J., Acworth, R.I., 2004. Analysis of the distribution of inorganic constituents in a landfill leachate-contaminated aquifer – Astrolabe Park, Sydney, Australia. Environmental Geology 46, 263–272.
Joseph, J.B., Cressey, G., Styles, J.R., Yuen, S.T.S., Cuadros, J., 2003. Observations of the impacts of some landfill leachates with clays. Environmental Technology 24, 419–428.
Kjeldsen, P., Bjerg, P.L., Rugge, K., Christensen, T.H., Pedersen, J.K., 1998. Characterization of an old municipal landfill (Grindsted, Denmark) as a groundwater pollution source. landfill hydrology and leachate migration. Waste Management & Research 16, 14–22.
Kjeldsen, P., Barlaz, M.A., Rooker, A.P., Baun, A., Ledin, A., Christensen, T.H., 2002. Present and long-term composition of MSW landfill leachate: a review. Critical Reviews in Environmental Science and Technology 32, 297–336.
Kulikowska, D., Klimiuk, E., 2008. The effect of landfill age on municipal leachate composition. Bioresource Technology 99, 5981–5985.
Lake, C.B., Rowe, R.K., 2005. The 14-year Performance of a Compacted Clay Liner used as Part of a Composite Liner System for a Leachate Lagoon. Geotechnical and Geological Engineering 23, 657–678.
Lee, J.Y., Cheon, J.Y., Kwon, H.P., Yoon, H.S., Lee, S.S., Kim, J.H., Park, J.K., Kim, C.G., 2006. Attenuation of landfill leachate at two uncontrolled landfills. Environmental Geology 51, 581–593.
Garcia, Lobo., de Cortazar, A., Tejero Monzon, I., 2007. MODUELO 2: a new version of an integrated simulation model for municipal solid waste landfills. Environmental Modelling & Software 22, 59–72.
Lyngkilde, J., Christensen, T.H., 1992a. Fate of organic contaminants in the redox zones of a landfill leachate pollution plume (Vejen, Denmark). Journal of Contaminant Hydrology 10, 291–307.
Lyngkilde, J., Christensen, T.H., 1992b. Redox zones of a landfill leachate pollution plume (Vejen, Denmark). Journal of contaminant hydrology 10, 273–289.
Marttinen, S.K., Kettunen, R.H., Rintala, J.A., 2003. Occurrence and removal of organic pollutants in sewages and landfill leachates. Science of the Total Environment 301, 1–12.
Marzougui, A., Ben Mammou, A., 2006. Impacts of the dumping site on the environment: Case of the Henchir El Yahoudia Site, Tunis, Tunisia. Comptes Rendus Geoscience 338, 1176–1183.
Meju, M.A., 2000. Geoelectrical investigation of old/abandoned, covered landfill sites in urban areas: model development with a genetic diagnosis approach. Journal of Applied Geophysics 44, 115–150.
Ministerio de Agricultura, Pesca y Alimentación, 1994. Métodos Oficiales de Análisis, Madrid.
Mohammadzadeh, H., Clark, I., Marschner, M., St-Jean, G., 2005. Compound specific isotopic analysis (CSIA) of landfill leachate DOC components. Chemical Geology 218, 3–13.
Moore, D.M., Reynolds, R.C., Jr., 1997. X - Ray Diffraction and the identification and analysis of clay minerals. Oxford University Press.
Mor, S., Ravindra, K., Dahiya, R.P., Chandra, A., 2006. Leachate characterization and assessment of groundwater pollution near municipal solid waste landfill site. Environmental Monitoring and Assessment 118, 435–456.
Morillas, P., Castello, R., Vizcayno, C., 2009. Laboratory alteration of gypsiferous materials below a landfill. Waste Management 29, 1359–1369.
Mostbauer, P., 2003. Criteria selection for landfills: do we need a limitation on inorganic total content. Waste Management 23, 547–554.
Munro, I.R.P., MacQuarrie, K.T.B., Valsangkar, A.J., Kan, K.T., 1997. Migration of landfill leachate into a shallow clayey till in southern New Brunswick: a field and modelling investigation. Canadian Geotechnical Journal 34, 204–219.
Nanny, M.A., Ratasuk, N., 2002. Characterization and comparison of hydrophobic neutral and hydrophobic acid dissolved organic carbon isolated from three municipal landfill leachates. Water Research 36, 1572–1584.
Owen, J.A., Manning, D.A.C., 1997. Silica in landfill leachates: implications for clay mineral stabilities. Applied Geochemistry 12, 267–280.
Primo, V., 2001, DRXWIN© vs 2.2.56, A Graphical and analytical tool for powder XRD Patterns.
Quigley, R.M., Fernandez, F., Yanful, E.K., Helgason, T., Margaritis, A., Whitby, J.L., 1987. Hydraulic conductivity of contaminated natural clay directly below a domestic landfill. Canadian Geotechnical Journal 24, 377–383.
Renou, S., Givaudan, J.G., Poulain, S., Dirassouyan, F., Moulin, P., 2008. Landfill leachate treatment: review and opportunity. Journal of Hazardous Materials 150, 468–493.
Rhoades, J.D., 1982. Cation exchange capacity. Methods of Soil analysis, American Society of Agronomy, Madison.
Rowe, R.K., Quigley, R.M., Booker John, R., 1995. Clayey Barrier Systems for Waste Disposal Facilities. Spon Press, Abingdon, Oxon.
Salem, Z., Hamouri, K., Djemaa, R., Allia, K., 2008. Evaluation of landfill leachate pollution and treatment. Desalination 220, 108–114.
Sanchez-Chardi, A., Nadal, J., 2007. Bioaccumulation of metals and effects of landfill pollution in small mammals. Part I. The greater white-toothed shrew, Crocidura russula. Chemosphere 68, 703–711.
Schultz, L.G., 1964. Quantitative interpretation of mineralogical composition from X-ray and chemical data for the Pierre Shale. U.S. Geological Survey professional paper 391-c, 1-31.
Shouliang, H., Beidou, X., Haichan, Y., H, L., Shilei, F., Hongliang, L., 2008. Characteristics of dissolved organic matter (DOM) in leachate with different landfill ages. Journal of Environmental Sciences-China 20, 492–498.
Spagni, A., Lavagnolo, M.C., Scarpa, C., Vendrame, P., Rizzo, A., Luccarini, L., 2007. Nitrogen removal optimization in a sequencing batch reactor treating sanitary landfill leachate. Journal of Environmental Science and Health Part A-Toxic/Hazardous Substances & Environmental Engineering 42, 757–765.
Srodon, J., Drits, V.A., McCarty, D.K., Hsieh, J.C.C., Eberl, D., 2001. Quantitative x-ray diffraction analysis of clay-bearing rocks from random preparations. Clays and Clay Minerals 49, 514–528.
Statom, R.A., Thyne, G.D., McCray, J.E., 2004. Temporal changes in leachate chemistry of a municipal solid waste landfill cell in Florida, USA. Environmental Geology 45, 982–991.
Straub, W.A., Lynch, D.R., 1982. Models of landfill leaching – moisture flow and inorganic strength. Journal of the Environmental Engineering Division-Asce 108, 231–250.
NA, S.W.A., 1997. Leachate generation, collection and treatment at municipal solid waste disposal facilities. Publication No. GR-D 0535 Solid waste association of North America. Silver Spring, Maryland.
Swati, M., Rema, T., Joseph, K., 2008. Hazardous organic compounds in urban municipal solid waste from a developing country. Journal of Hazardous Materials 160, 213–219.
Tatsi, A.A., Zouboulis, A.I., 2002. A field investigation of the quantity and quality of leachate from a municipal solid waste landfill in a Mediterranean climate (Thessaloniki, Greece). Advances in Environmental Research 6, 207–219.
Taylor, R., Allen, A. 2006. Waste disposal and landfill: information needs. In: Schmoll, O., Howard, G., Chilton, J., Chorus, I. (Eds.), Protecting Groundwater for Health: Managing the Quality of Drinking-water Sources, London.
Techer, I., Lancelot, J., Clauer, N., Liotard, J.M., Advocat, T., 2001. Alteration of a basaltic glass in an argillaceous medium: The Salagou dike of the Lodeve Permian Basin (France). Analogy with an underground nuclear waste repository. Geochimica Et Cosmochimica Acta 65, 1071–1086.
Tejero, I., Szanto, M., Fantelli, M., Diaz, R., 1991. Caracterización y tratabilidad de los lixiviados de vertederos de residuos sólidos urbanos: caso del vertedero de Meruelo. Retema: revista técnica del medio ambiente 25, 111–118.
Thomas, G.W., 1982. Exchangeable cations. In: Methods of Soil Analysis, second ed. American Society of Agronomy, Madison.
Thornton, S.F., Lerner, D.N., Tellam, J.H., 2001. Attenuation of landfill leachate by clay liner materials in laboratory columns: 2. Behaviour of inorganic contaminants. Waste Management & Research 19, 70–88.
Yanful, E.K., Quigley, R.M., Nesbitt, H.W., 1988. Heavy metal migration at a landfill site, Sarnia, Ontario, Canada—2: metal partitioning and geotechnical implications. Applied Geochemistry 3, 623–629.
Vadillo, I., Carrasco, F., Andreo, B., de Torres, A.G., Bosch, C., 1999. Chemical composition of landfill leachate in a karst area with a Mediterranean climate (Marbella, southern Spain). Environmental Geology 37, 326–332.
van Breukelen, B.M., Griffioen, J., Roling, W.F.M., van Verseveld, H.W., 2004. Reactive transport modelling of biogeochemical processes and carbon isotope geochemistry inside a landfill leachate plume. Journal of Contaminant Hydrology 70, 249–269.
Xie, H.J., Chen, Y.M., Zhan, L.T., Chen, R.P., Tang, X.W., Chen, R.H., Ke, H., 2009. Investigation of migration of pollutant at the base of Suzhou Qizishan landfill without a liner system. Journal of Zhejiang University-Science A 10, 439–449.
Zairi, M., Ferchichi, M., Ismail, A., Jenayeh, M., Hammami, H., 2004. Rehabilitation of El Yahoudia dumping site, Tunisia. Waste Management 24, 1023–1034.